

Structure–Activity Relationships of the Cycloalkanol Ethylamine Scaffold: Discovery of Selective Norepinephrine Reuptake Inhibitors

Paige E. Mahaney,^{*,§} Lori K. Gavrín,[§] Eugene J. Trybulski,[§] Gary P. Stack,[†] An T. Vu,[§] Stephen T. Cohn,^{§,‡} Fei Ye,[§] Justin K. Belardi,[§] Arthur A. Santilli,[§] Joseph P. Sabatucci,[§] Jennifer Leiter,[†] Grace H. Johnston,^{†,‡} Jenifer A. Bray,[†] Kevin D. Burroughs,^{†,‡} Scott A. Cosmi,[†] Liza Leventhal,^{#,×} Elizabeth J. Koury,[†] Yingru Zhang,^{§,∞} Cheryl A. Muford,^{||} Douglas M. Ho,^{∇,△} Sharon J. Rosenzweig-Lipson,[#] Brian Platt,[#] Valerie A. Smith,[#] and Darlene C. Deecher[†]

Chemical and Screening Sciences, Women's Health and Musculoskeletal Biology, and Drug Safety and Metabolism, Wyeth Research, 500 Arcola Road, Collegeville, Pennsylvania 19426, Chemical and Screening Sciences and Department of Neuroscience, Wyeth Research, CN 8000, Princeton, New Jersey 08543, and Department of Chemistry, Princeton University, Princeton, New Jersey 08544

Received March 3, 2008

Further exploration of the cycloalkanol ethylamine scaffold, of which venlafaxine (**1**) is a member, was undertaken to develop novel and selective norepinephrine reuptake inhibitors (NRIs) for evaluation in a variety of predictive animal models. These efforts led to the discovery of a piperazine-containing analogue, **17g** (WY-46824), that exhibited potent norepinephrine reuptake inhibition, excellent selectivity over the serotonin transporter, but no selectivity over the dopamine transporter. Synthesis and testing of a series of cyclohexanol ethylpiperazines identified (*S*)-(-)-**17i** (WAY-256805), a potent norepinephrine reuptake inhibitor (IC₅₀ = 82 nM, K_i = 50 nM) that exhibited excellent selectivity over both the serotonin and dopamine transporters and was efficacious in animal models of depression, pain, and thermoregulatory dysfunction.

Introduction

Norepinephrine (NE^a), a major neurotransmitter, is released from noradrenergic neurons during synaptic transmission. Noradrenergic neurons project from the locus coeruleus to stimulate stress responses^{1c,d} and arousal^{1a,b} and to regulate the sympathetic nervous system.^{1d,e} These neurons modulate nearly all areas of the brain including the hippocampus, which is involved in memory and learning,² the prefrontal cortex, which is involved in drive and motivation,³ and the hypothalamus, which is involved in temperature regulation and sleep.⁴ NRIs enhance the transmission of NE by increasing its synaptic availability through blockage of its reuptake by the norepinephrine transporter (NET), making NRIs potential treatments for a wide range of disorders. Compounds that block both NE and serotonin (5-HT) reuptake, such as venlafaxine (**1**), duloxetine (**2**), and

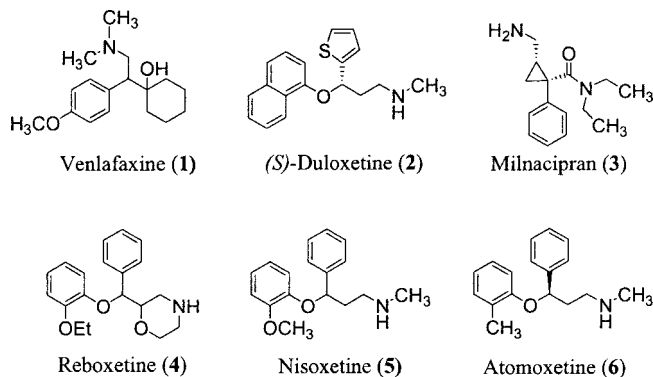


Figure 1. Chemical structures of marketed SSRIs, SNRIs, and NRIs.

milnacipran (**3**), Figure 1, have been approved in the U.S. and in Europe for indications including major depressive disorder (MDD) and pain disorders such as diabetic neuropathy. In addition, compounds with this profile have been reported to exhibit efficacy for other ailments such as stress urinary incontinence (SUI),⁵ attention deficit hyperactivity disorder (ADHD),⁶ and fibromyalgia.⁷ Drugs that selectively inhibit norepinephrine reuptake, including reboxetine (**4**) and nisoxetine (**5**), are marketed for the treatment of MDD; more recently, atomoxetine (**6**) was approved for the treatment of ADHD. Interestingly, although atomoxetine has little affinity for the dopamine transporter (DAT), it has been shown to selectively increase extracellular dopamine levels in the prefrontal cortex without a concomitant increase in either the nucleus accumbens or striatum.⁸ Reboxetine and atomoxetine have also been reported to show efficacy for chronic pain disorders such as fibromyalgia⁹ and low back pain.^{9a}

Background

Venlafaxine (**1**), a member of the cycloalkanol ethylamine scaffold, was the first dual-acting serotonin and norepinephrine reuptake inhibitor (SNRI) to be approved for the treatment of

* To whom correspondence should be addressed. Phone: 484-865-0627. Fax: 484-865-9399. E-mail: mahanep@wyeth.com.

[§] Chemical and Screening Sciences, Wyeth Research, PA.

[†] Chemical and Screening Sciences, Wyeth Research, NJ.

[‡] Current address: Encysive Pharmaceuticals Inc., Houston, TX 77030.

[†] Women's Health and Musculoskeletal Biology, Wyeth Research, PA.

[‡] Current address: Neotropix, Inc., Malvern, PA 19355.

[#] Department of Neuroscience, Wyeth Research, NJ.

[×] Current address: EnVivo Pharmaceuticals, Watertown, MA 02472.

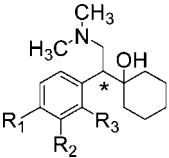
[∞] Current address: Bristol-Myers Squibb Pharmaceutical Research Institute, Princeton, NJ 08543.

^{||} Drug Safety and Metabolism, Wyeth Research, PA.

[∇] Current address: Department of Chemistry, Harvard University, Cambridge, MA 02138.

[△] Department of Chemistry, Princeton University.

^a Abbreviations; NRI, norepinephrine reuptake inhibitor; NE, norepinephrine; NET, norepinephrine transporter; 5-HT, serotonin; MDD, major depressive disorder; SUI, stress urinary incontinence; ADHD, attention hyperactivity disorder; SNRI, serotonin and norepinephrine reuptake inhibitor; SAR, structure–activity relationship; hNET, human norepinephrine transporter; hSERT, human serotonin transporter; cpm, counts per minute; MDCK, Madin–Darby canine kidney; hDAT, human dopamine transporter; BOP, benzotriazol-1-ylxytris(dimethylamino)phosphonium hexafluorophosphate; THF, tetrahydrofuran; SSRI, selective serotonin reuptake inhibitor; SRI, serotonin reuptake inhibitor; ip, intraperitoneal; sc, subcutaneous; po, oral; AUC, area under the curve; C_{max}, maximum concentration; OVX, ovariectomized; TST, tail-skin temperature.

Table 1. Characterization of Cyclohexanol Ethyl *N,N'*-dimethylamine Analogues at the Human Norepinephrine, Serotonin, and Dopamine Transporters^a


compd	R ₁	R ₂	R ₃	hNET binding, ^b K _i (StDev), nM	hNET uptake, ^c IC ₅₀ (StDev) [rNET uptake], ¹⁰ nM	hSERT uptake, ^d IC ₅₀ (StDev) [rSERT uptake], ¹⁰ nM	ratio of (hSERT uptake IC ₅₀ , nM)/(hNET uptake IC ₅₀ , nM) ^e	hDAT binding inhibition ^f (StDev), %
1	OCH ₃	H	H	385 (103)	535 (64) [640]	31 (4) [210]	0.05	45 ^h (2)
7	H	OCH ₃	H	316 (108)	208 (16) [620]	88 (34) [190]	0.42	9 ^g
8	Cl	H	H	249 (121)	120 (1) [300]	123 (88) [180]	1.0	23 ^g
9	H	Cl	H	149 (40)	121 (45) [160]	292 (115) [320]	2.4	28 ^g
10	H	H	Cl	125 (49)	205 (119) [NR]	177 (127) [NR]	0.86	13 ^g
11	H	CF ₃	H	21 (12)	32 (7) [360]	534 (62) [1440]	16.7	15 ^g
(<i>R</i>)-(-)- 9	H	Cl	H	41 (18)	46 (13)	405 (99)	8.8	17 ^g
(<i>S</i>)-(+)- 9	H	Cl	H	339 (100)	303 (46)	155 (78)	0.51	0 ^g

^a Data are the average of at least two independent experiments, each run in triplicate. NR means the data were not previously reported. ^b Inhibition of [³H]nisoxetine binding to MDCK-Net6 cells stably transfected with hNET. Desipramine (K_i = 2.1 ± 0.6 nM) was used as a standard. K_i = IC₅₀/(1 + [L]/K_D), where [L] equals concentration of radioligand added. ^c Inhibition of NE uptake in MDCK-Net6 cells stably transfected with hNET. Desipramine (IC₅₀ = 3.4 ± 1.6 nM) was used as a standard. ^d Inhibition of 5-HT uptake in JAR cells stably transfected with hSERT. Fluoxetine (IC₅₀ = 9.4 ± 3.1 nM) was used as a standard. ^e Unitless value as a ratio in which higher numbers represent relatively greater NET selectivity. A value of 1 represents no selectivity. ^f Inhibition of radioligand **18** binding to membranes from CHO cells expressing recombinant hDAT. Mazindol (22.1 ± 6.5 nM) was used as a standard. ^g Percent inhibition measured at a concentration of 1000 nM. ^h Percent inhibition measured at a concentration of 10 000 nM.

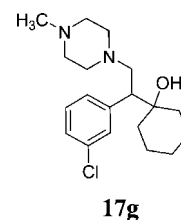
MDD and continues to be widely prescribed. A drug discovery program was initiated to re-examine the structure–activity relationship (SAR) within the cycloalkanol ethylamine scaffold to identify novel and selective NRIs for in vivo evaluation in a panel of predictive animal models. Our initial strategy involved screening libraries of in-house compounds that were originally prepared for the historical MDD program. This approach entailed retesting compounds using a cell line expressing the human norepinephrine transporter (hNET), since uptake inhibition of NE and 5-HT was previously evaluated in rat brain cortical synaptosomes as reported in the original cycloalkanol ethylamine paper.¹⁰ According to a new paradigm, compounds were screened in vitro in MDCK-Net6 cells that were stably transfected with hNET. These cells were then treated with the test compound followed by [³H]NE to initiate NE uptake. Once the cells were washed and lysed, uptake of [³H]NE was measured by collection of counts per minute (cpm) data. Serotonin uptake into JAR cells that were stably transfected with the human serotonin transporter (hSERT) was similarly measured. Binding affinity for hNET was determined using a competition radioligand-binding assay in whole MDCK cells with [³H]nisoxetine as the radioligand. Previous studies with cycloalkanol ethylamine analogues revealed a significant reduction in binding affinity using purified membranes versus whole cells.¹¹ In addition, values from the whole cell assay more closely correlated to inhibition of NE uptake.¹¹ Affinity for hNET was compared to affinity for the human dopamine transporter (hDAT) measured using purified CHO membranes expressing recombinant hDAT. The cocaine analogue, [³H]-3β-(4-fluorophenyl)tropane-2β-carboxylic acid methyl ester¹² (**18**, [³H]WIN35,428) was used as the radioligand. Target in vitro profiles for drug candidates included an IC₅₀ value of less than 100 nM in the hNET uptake assay and selectivity over hSERT and hDAT of greater than 100-fold.

A set of original cyclohexanol ethyl *N,N'*-dimethylamines, chosen to examine the effect of aromatic ring substitution on selectivity and potency, was characterized for activity at the human monoamine transporters (Table 1). Good agreement was observed between the previously reported SAR established in rat cortical synaptosomes¹⁰ and that determined in cells transfected with the human transporters; however, the absolute IC₅₀ values differed for some compounds. In general, increasing the

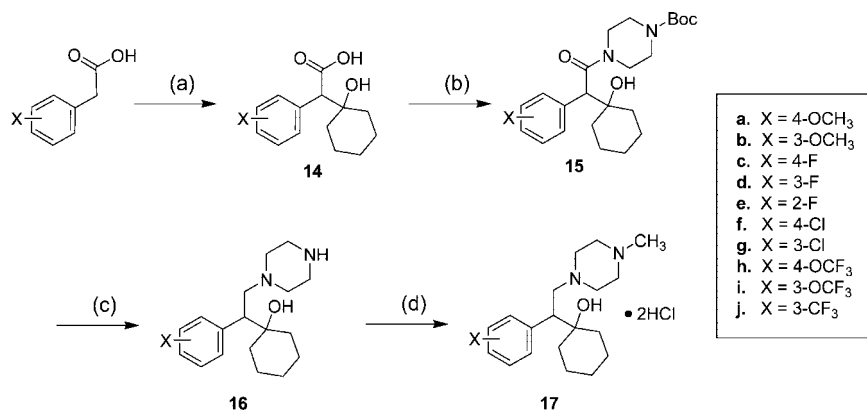
electron-withdrawing nature of the aromatic ring provided more potent inhibitors of NE uptake and improved the selectivity for NET over SERT. For example, substitution with a *p*-methoxy group (compound **1**) provided the weakest NRI (535 nM) and was 17-fold more potent at inhibiting 5-HT uptake. The *m*-chloro analogue (**9**) had an intermediate IC₅₀ value of 149 nM in the NE uptake assay and exhibited 2.4-fold selectivity over SERT, while the strongest electron-withdrawing *m*-trifluoromethyl analogue (**11**) was the most potent inhibitor of NE uptake, with an IC₅₀ value of 32 nM, and exhibited the best selectivity over 5-HT uptake, nearly 17-fold. All compounds tested exhibited only weak binding to hDAT.

The effect of stereochemistry on selectivity and potency of the series was examined by separating compound **9** into its enantiomers using chiral HPLC. Assignment of the stereochemistry was based upon analogy to (*S*)-(+)-venlafaxine, which was unequivocally established previously via single-crystal X-ray diffraction.¹⁰ The *R*-enantiomer of **9** exhibited an increase in both potency for hNET and selectivity over hSERT when compared to its racemate, while the *S*-enantiomer was both less potent and selective versus the racemate. Interestingly, hSERT had a potency preference for the *S*-enantiomer, which was opposite to that observed for hNET.

Since variation of aromatic substitution in the cyclohexanol ethyl *N,N'*-dimethylamine series did not provide compounds that met selectivity criteria for hNET over hSERT, additional examples within the cycloalkanol ethylamine scaffold with varied amine moieties were screened. These efforts led to the identification of a piperazine-containing analogue, **17g** (WY-46824), as a potent NRI (IC₅₀ = 58 nM, hNET K_i = 46 nM)



that exhibited nearly 300-fold selectivity over hSERT. Unfortunately, this compound had high affinity for hDAT (K_i = 53 nM), which was an undesired target for the purposes of this

Scheme 1. Synthesis of Cycloalkanol Ethylamine Analogues^a

^a Reagents: (a) LDA (2.5 equiv), THF, -78 °C to room temp, then cyclohexanone, -78 °C (83–99%); (b) BOP reagent, 1-Boc-piperazine, CH_2Cl_2 (59–87%); (c) BH_3 -THF, reflux, then aqueous HCl (51–69%); (d) HCHO, HCO_2H , H_2O , then HCl/MeOH (58–79%).

program. Therefore, new piperazine-containing analogues were synthesized with the goal of eliminating affinity for hDAT while maintaining the potency for hNET and selectivity over hSERT that was exhibited by the lead compound (**17g**).

Chemistry

A parallel synthesis approach for the generation of new analogues in the cyclohexanol ethylpiperazine scaffold was evaluated. The published synthetic route¹⁰ was not deemed suitable for parallel synthesis because of a tendency toward retroaldol and low isolable yields obtained when the aldol reaction was conducted on the starting phenylacetic amide. Consequently, an improved synthesis that was amenable to a parallel approach was developed (Scheme 1). Performing the aldol reaction on the dianion of the starting phenylacetic acid at -78 °C prevented the occurrence of the reverse aldol reaction and gave the desired product in high yield. In contrast, quenching the aldol product at 0 °C, instead of maintaining a temperature of -78 °C, resulted in the isolation of a significant amount of starting material, presumably due to the retroaldol mechanism. Amine coupling to aldol product **14** to form amide **15** could be accomplished with a variety of conventional agents; however, benzotriazol-1-yloxytris(dimethylamino)phosphonium hexafluorophosphate (BOP reagent) was selected because of its ease of handling and good yields obtained in parallel reactions. Reduction of the amide with borane-THF complex at elevated temperatures followed by in situ deprotection with hydrochloric acid afforded cycloalkanol amine analogues **16**, which could be N-methylated with an aqueous solution of formaldehyde in formic acid to afford N-methylpiperazine analogues **17**. Amines **16** and **17** were converted to dihydrochloride salts using methanolic hydrochloric acid prior to in vitro characterization.

The enantiomers of compounds **16g**, **17g**, **16i**, and **17i** were prepared in >99.5% optical purity via separation of the Boc-protected amide intermediates **15g** and **15i** using chiral supercritical fluid chromatography. Attempts to separate the enantiomers of either **16g** or **17g** afforded products with significantly reduced optical purity. Assignment of the absolute configuration of (*R*)-(+)-**17g** was unequivocally established by a single-crystal X-ray analysis (Figure 2). Assignment of the stereochemistry of **16g**, **16i**, and **17i** was based upon analogy.

Results and Discussion

In Vitro Characterization. The cyclohexanol ethylpiperazine analogues were characterized in vitro for their activity at the human monoamine transporters (Table 2). The effect of aromatic

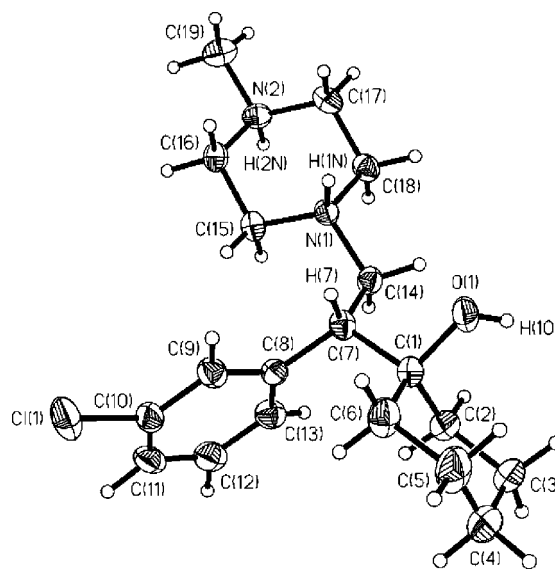
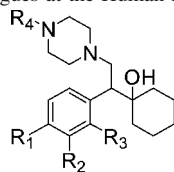


Figure 2. ORTEP view of 1-[(1*R*)-1-(3-chlorophenyl)-2-(4-methylpiperazin-1-yl)ethyl]cyclohexanol [(*R*)-(+)-**17g**].

substitution on the SAR for reuptake inhibition at hNET in this series was similar to that seen within the *N,N'*-dimethylamine class. Again, the *p*-methoxy analogues (**16a** and **17a**) were the weakest inhibitors of NE uptake while the *m*-chloro (compounds **16g** and **17g**) and the *m*-trifluoromethyl analogues (**16j** and **17j**) were the most potent. Differing slightly, however, from the *N,N'*-dimethylamine SAR, in which the *m*-trifluoromethyl analogue **11** was preferred over the *m*-chloro analogue **9** for NRI potency and selectivity over hSERT, was the observation that within the cyclohexanol ethylpiperazines the *m*-chloro substituent (**16g**, **17g**) provided equivalent or improved potency and affinity at hNET versus the *m*-trifluoromethyl analogues (**16j**, **17j**). Interestingly, all analogues containing the *m*-chloro group also exhibited high affinity for hDAT while the trifluoromethyl analogues did not. To further explore this observation, the *m*-trifluoromethoxy analogues **16i** and **17i** were synthesized. These compounds also maintained good potency and affinity at hNET while possessing very little affinity for hDAT. In contrast, the *m*-methoxy analogue (compound **17b**) exhibited significantly reduced activity at all transporters.

N-Methylation of the piperazine ring had no significant impact in vitro on hNET potency and affinity. For example, a comparison of the two racemic *m*-trifluoromethoxy analogues revealed IC_{50} values for NE uptake of 147 nM for *N*-

Table 2. Characterization of Cyclohexanol Ethylpiperazine Analogues at the Human Norepinephrine, Serotonin, and Dopamine Transporters^a

compd	R ₁	R ₂	R ₃	R ₄	hNET binding, ^b K _i (StDev), nM	hNET uptake, ^c IC ₅₀ (StDev), nM	hSERT uptake, ^d IC ₅₀ (StDev), nM	hDAT binding, ^e K _i (StDev), nM	hDAT binding inhibition at 1 μM ^f (StDev), %
17a	OCH ₃	H	H	CH ₃		34% (18) ^{f,g}	11% ^f (13)		5
16a	OCH ₃	H	H	H	519 (233)	34% (1) ^{f,g}	24% ^f (8)		9
17b	H	OCH ₃	H	CH ₃	514 (339)	600 (143)	14% ^f (16)		4
16b	H	OCH ₃	H	H	745 (248)	870 (126)	8% ^f (6)		2
17c	F	H	H	CH ₃	1376 (738)	1452 (73)	13% ^f (4)		32
16c	F	H	H	H	1034 (394)	1499 (242)	29% ^f		22
17d	H	F	H	CH ₃	364 (167)	240 (160)	12% ^f		29 ^g
16d	H	F	H	H	368 (211)	673 (66)	12% ^f		22
17e	H	H	F	CH ₃	34% ^{f,g}	19% ^f			
16e	H	H	F	H	38% ^{f,g}	31% ^{f,g}			
17f	Cl	H	H	CH ₃	1220 (266)	7% ^f	0% ^f		26
16f	Cl	H	H	H	717 (95)	29% ^{f,g}	1525 (322)		35
17g	H	Cl	H	CH ₃	46 (3)	58 (10)	18795 (4600)	53 (18)	
(<i>R</i>)-(+)- 17g	H	Cl	H	CH ₃	187 (51)	577 (103)	0% ^f	235 (50)	
(<i>S</i>)-(–)- 17g	H	Cl	H	CH ₃	14 (8)	29 (5)	9% ^f	73 (35)	
16g	H	Cl	H	H	18 (11)	38 (14)	4962 (423)	45 (17)	
(<i>R</i>)-(–)- 16g	H	Cl	H	H	214 (87)	540 (26)	6102 (749)	340 (63)	
(<i>S</i>)-(+)- 16g	H	Cl	H	H	17 (4)	25 (7)	2669 (175)	135 (30)	
17h	OCF ₃	H	H	CH ₃	417 (131)	575 (162)	1214 (99)		13 (9)
17i	H	OCF ₃	H	CH ₃	91 (58)	147 (87)	12% ^f (14)		3% (11)
(<i>R</i>)-(+)- 17i	H	OCF ₃	H	CH ₃	785 (488)	3474 (313)	4% ^f		5 (7)
(<i>S</i>)-(–)- 17i	H	OCF ₃	H	CH ₃	50 (8)	82 (21)	3% ^f		6 (1)
16i	H	OCF ₃	H	H	140 (89)	284 (93)	3% ^f		13 (5)
(<i>R</i>)-(–)- 16i	H	OCF ₃	H	H	544 (232)	1290 (110)	11% ^f (15)		15 (6)
(<i>S</i>)-(+)- 16i	H	OCF ₃	H	H	117 (41)	140 (82)	3% ^f		13 (12)
17j	H	CF ₃	H	CH ₃	61 (10)	92 (6)	28% ^{f,g}		6
16j	H	CF ₃	H	H	58 (14)	94 (17)	13% ^f		4

^a Data are the average of at least three independent experiments, each run in triplicate. ^b Inhibition of [³H]nisoxetine binding to MDCK-Net6 cells stably transfected with hNET. Desipramine (K_i = 2.1 ± 0.6 nM) was used as a standard. K_i = IC₅₀/(1 + [L]/K_D), where [L] equals concentration of radioligand added. ^c Inhibition of NE uptake in MDCK-Net6 cells stably transfected with hNET. Desipramine (IC₅₀ = 3.4 ± 1.6 nM) was used as a standard. ^d Inhibition of serotonin uptake in JAR cells stably transfected with human SERT. Fluoxetine (IC₅₀ = 9.4 ± 3.1 nM) was used as a standard. ^e Inhibition of radioligand **18** binding to membranes from CHO cells expressing recombinant hDAT. Mazindol (22.1 ± 6.5 nM) was used as a standard. ^f Percent inhibition measured at a concentration of 1000 nM. ^g Compound gave poor dose response; therefore, no IC₅₀ was obtained.

methylpiperazine **17i** compared to 284 nM for the unsubstituted analogue (**16i**). Likewise, *m*-trifluoromethyl analogues **16j** and **17j** had essentially identical IC₅₀ values of 92 and 94 nM, respectively.

While the effect of aromatic substitution on the SAR for reuptake inhibition at hNET in the cyclohexanol ethylpiperazine series was similar to that seen within the *N,N'*-dimethylamine class, a major difference was observed for 5-HT uptake inhibition. In general, the electronic nature of the aromatic ring had little effect because incorporation of a piperazine ring into the scaffold essentially eliminated 5-HT reuptake inhibitory activity. For example, the *N*-methylpiperazine analogue containing a *p*-methoxy substituent (**17a**), the most potent substituent for 5-HT uptake inhibition in the *N,N'*-dimethylamine series, exhibited only 11% inhibition of hSERT at 1 μM. Among the cyclohexanol ethylpiperazines that were synthesized, the most potent SRIs (compounds **16f** and **17h**) had IC₅₀ values of greater than 1 μM.

The effect of stereochemistry on the selectivity and potency of this series was examined by testing the enantiomeric pairs of compounds **16g**, **17g**, **16i**, and **17i**. In all four examples, the *S*-enantiomer was the eutomer, exhibiting an increase in both functional potency and binding affinity at hNET compared to the corresponding racemate while the *R*-enantiomer was significantly less active. For example, in the NE uptake assay, (*S*)-(–)-**17g** had an IC₅₀ value of 29 nM (K_i value of 14 nM in the binding assay) while (*R*)-(+)-**17g** exhibited an IC₅₀ of 577 nM

(K_i value of 187 nM in the binding assay). This is a striking reversal from the preferred stereochemistry seen in the cyclohexanol ethyl *N,N'*-dimethylamine series where the *R*-enantiomer was the eutomer. A future publication will examine this intriguing observation in detail. Unfortunately for the *m*-chloro derivatives, the preferred stereochemistry for both hDAT and hNET was the *S*-enantiomer; consequently, no additional selectivity for hNET over hDAT was achieved through resolution. However, among the *m*-trifluoromethoxy derivatives, (*S*)-(–)-**17i** (WAY-256805) was a potent NRI (IC₅₀ value of 82 nM, K_i value of 50 nM) that was highly selective over both hSERT and hDAT. This compound was selected for further evaluation.

The potential for cross-reactivity of (*S*)-(–)-**17i** with 5-HT and adrenergic receptors was assessed using either a calcium mobilization assay measured on a fluorometric imaging plate reader (FLIPR) testing for both agonists and antagonists or a competition radioligand-binding assay. (*S*)-(–)-**17i** exhibited IC₅₀ and EC₅₀ values of greater than 10 μM across all receptors. Test receptors included 5-HT_{1B}, 5-HT_{1D}, 5-HT_{2A}, 5-HT_{2B}, 5-HT₆, 5-HT₇, and adrenergic receptor 1α.

In Vivo Characterization. The antidepressant-like effects of compound (*S*)-(–)-**17i** were assessed in the mouse tail-suspension model.^{13a} During testing, subsequent to compound administration, male mice were suspended upside down by their tails and movements of the animals during a 6 min test session were automatically recorded. These movements were classified

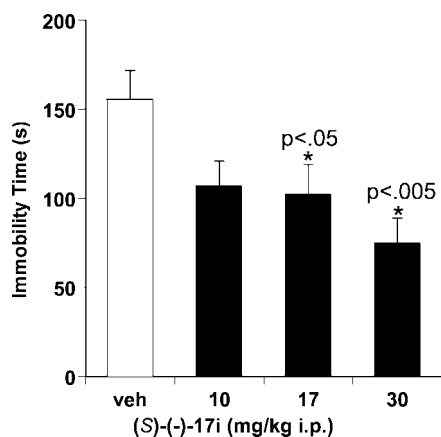


Figure 3. Effect of (S)-(-)-17i in the tail-suspension test in male mice. A vehicle of 2% Tween-80/0.5% methylcellulose in water was used for delivery of test compounds. Data represent group mean \pm SEM for each dose ($N = 10$ per group).

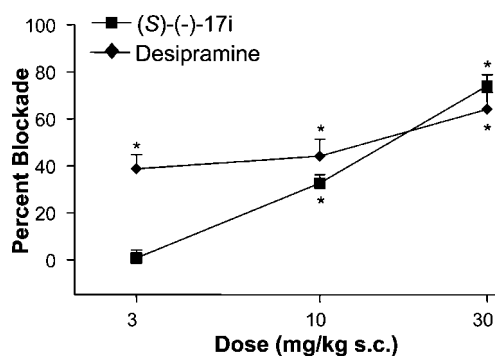


Figure 4. Effect of (S)-(-)-17i in the mouse *p*-phenylquinone model of acute visceral (abdominal) pain. A vehicle of saline was used for dosing. Data are presented as percent blockade compared to vehicle (% blockade = [(mean vehicle) - (drug)]/(mean vehicle) \times 100) \pm SEM for each dose ($N = 8$ per group); * signifies a p value of < 0.05 vs saline vehicle (ANOVA).

into periods of agitation (i.e., efforts to regain footing) and immobility. A decrease in immobility time in this model has been reported to correspond with antidepressant-like activity.¹³ As shown in Figure 3, when administered via intraperitoneal injection (ip) (S)-(-)-17i significantly decreased immobility time, with a p value of < 0.05 (ANOVA), at 17 and 30 mg/kg, 38% and 53%, respectively, in a dose-dependent manner indicating antidepressant activity. Desipramine, a classical tricyclic antidepressant with selectivity for NET, has been reported to reduce immobility time in this model 25% and 30% when administered ip at doses of 8 and 16 mg/kg, respectively.¹⁴

The antinociceptive effects of (S)-(-)-17i were evaluated in a mouse *p*-phenylquinone model of acute visceral (abdominal) pain.¹⁵ In this model, *p*-phenylquinone, administered via ip injection, acts as a localized irritant resulting in an abdominal constriction response (i.e., writhing) which can be quantified. The ability of a compound to reduce the number of abdominal constrictions predicts efficacy toward attenuating visceral pain. The role of NE, a major component of the endogenous descending pain inhibitory system from the rostral ventral medulla to the spinal cord,¹⁶ has been formerly characterized.¹⁷ Our dose-response data for desipramine have been previously described in this model at doses between 1 and 30 mg/kg.¹⁸ Figure 4 shows the effect of (S)-(-)-17i compared to desipramine, after subcutaneous (sc) administration between 3 and 30 mg/kg. Compound (S)-(-)-17i significantly reduced the

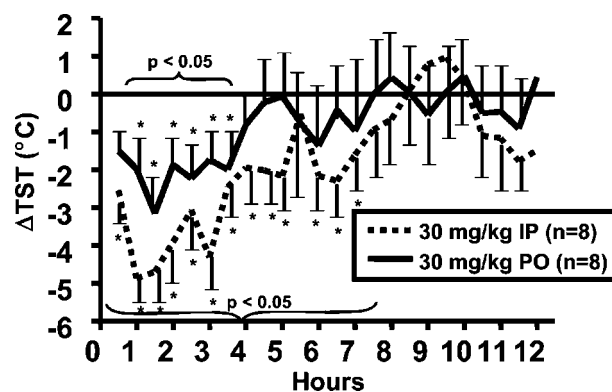


Figure 5. Effect of ip and po administration of (S)-(-)-17i in a telemetric rat model of ovariectomized (OVX)-induced thermoregulatory dysfunction; * signifies a p value of < 0.05 vs 2% Tween-80 /0.5% methylcellulose in water vehicle. The onset of an effect was defined as the first half-hour interval of two consecutive significant ($p < 0.05$) half-hour intervals. The treatment effect was defined to have ended when there are two consecutive nonsignificant ($p \geq 0.05$) half-hour intervals. Braces mark periods of significant effects. Error bars represent standard error of the mean of each data point.

number of abdominal constrictions when compared to vehicle ($p < 0.05$, ANOVA) at 10 and 30 mg/kg with similar efficacy as desipramine at both doses. While efficacy was similar between the two compounds, not surprisingly, desipramine was more potent, exhibiting significant activity at doses down to 1 mg/kg,¹⁸ consistently reflecting the *in vitro* 25-fold difference in potency.

NE has been reported to stimulate areas of the hypothalamus that play an important role in temperature regulation.⁴ In order to determine its effects on temperature homeostasis, compound (S)-(-)-17i was also evaluated in a telemetric rat model of ovariectomized (OVX)-induced thermoregulatory dysfunction.¹⁹ Intact cycling rats exhibit a diurnal rhythm during which, over a 24 h period, their tail-skin temperature (TST) decreases during the dark (active) phase and remains elevated during the light (inactive) phase. Reduction in ovarian hormones as a result of ovariectomy causes the TST of OVX-rats to remain elevated during both the dark and light phases, and treatment with estrogen has been reported to restore the normal diurnal temperature pattern to that seen in an intact rat.^{19a} Results of the evaluation of both SSRIs and SNRIs in this model have been previously reported;²⁰ however, activity of a selective NRI has not been described. According to our published paradigm,²¹ test compounds, administered 30 min prior to the dark phase, were analyzed for their ability to reduce TST versus baseline (individual baselines are measured for vehicle-dosed rats 1 day prior to administration of compound). TST was measured with a temperature and physical activity transmitter implanted sc with the tip of the temperature probe tunneled 2.5 cm beyond the base of the tail. Results for (S)-(-)-17i administered at a dose of 30 mg/kg both ip and orally (po) are depicted in Figure 5. Both routes of administration resulted in significant reductions of TST; however, ip administration achieved both a larger absolute reduction of TST and a longer duration of action when compared to po administration (Table 3). To help understand this difference in activity, the female rat pharmacokinetic parameters were measured (Table 4). A significant difference in both the maximum concentration (C_{max}) and the area under the curve (AUC) with (S)-(-)-17i in rats in the two routes of administration was observed. The C_{max} after ip administration

Table 3. Summary of (S)-(-)-**17i** in a Telemetric Rat Model of OVX-Induced Thermoregulatory Dysfunction Dosed po and ip (30 mg/kg)

route of administration of (S)-(-)- 17i (dose)	onset of activity vs baseline ($p < 0.05$), h	duration of action, h	mean reduction in TST from baseline, °C	maximum reduction in TST from baseline, °C
po (30 mg/kg)	1	3	-2.16	-3.15
ip (30 mg/kg)	0.5	6.5	-2.75	-4.87

Table 4. Female Sprague–Dawley (SD) Rat Pharmacokinetic Parameters for Compound (S)-(-)-**17i** after ip and po Dosing^a

route of administration	dose, mg/kg	C_{\max} , ng/mL	$t_{1/2}$, h	AUC _{0-inf} , ng·h/mL
ip ^b	30	2686 (442)	2.3 (0.5)	6163 (362)
po ^b	30	324 (131)	1.6 (0)	931 (310)

^a Numbers in parentheses are standard deviations of $n = 3$ animals.

^b Compound was dosed in 2% Tween-80/0.5% methylcellulose in water as the vehicle.

was 8-fold higher than after po administration, while the AUC values differed by nearly 7-fold.

Summary

Efforts to identify selective and potent NRIs from the cycloalkanol ethylamine scaffold, of which venlafaxine (**1**) is a member, provided a piperazine-containing class of compounds that is highly selective for hNET over hSERT. Replacement of the *m*-chloro group in the lead compound (**17g**) with a fluorine-containing electron-withdrawing group such as trifluoromethoxy or trifluoromethyl afforded potent NRIs with excellent selectivity over both hDAT and hSERT. Further investigation of the effect of (S)-(-)-**17i** in animals revealed it to be efficacious in models of depression, acute visceral pain, and thermoregulatory dysfunction.

Experimental Section

General Methods. Solvents were purchased as anhydrous grade and were used without further purification. Melting points were measured on a Mel-Temp II (Laboratory Device, Inc.) melting point apparatus and are uncorrected. ¹H NMR spectra were recorded on a Varian INOVA 400 instrument, and chemical shifts are reported in δ values (parts per million, ppm) relative to an internal standard tetramethylsilane in CDCl₃ or DMSO-*d*₆. In all cases, NMR spectra of enantiomers were essentially identical to those of their corresponding racemates. Electrospray (ESI) mass spectra were recorded using a Waters Alliance-ZMD mass spectrometer. Electron impact ionization (EI, EE = 70 eV) mass spectra were recorded on a Finnigan Trace mass spectrometer. Combustion analyses were performed by Robertson Microlit. Analytical thin layer chromatography (TLC) was performed on precoated plates (silica gel, 60 F-254) and were visualized using UV light and/or staining with a phosphomolybdic acid solution in ethanol. Optical rotations of individual enantiomers were obtained on a JASCO P-1020 polarimeter using a 1.0 mL microcell and methanol as the solvent. In general, compound purity was assessed by ¹H NMR and either a LC/UV/MS method or an analytical HPLC method as described in Supporting Information. Biological results were obtained on compounds of >97% chemical purity as determined by the above methods. The syntheses of **1** and **7–11** have been previously described.¹⁰

1-[(1R)-1-(3-Chlorophenyl)-2-(dimethylamino)ethyl]cyclohexanol [(R)-(-)-9**].** Racemic 1-(1-(3-chlorophenyl)-2-(dimethylamino)ethyl)cyclohexanol **9**¹⁰ was dissolved in methanol at a concentration of approximately 40 mg/mL, and the resulting solution was injected onto the supercritical fluid chromatography (SFC) instrument with a volume of 1.0 mL per injection. The baseline resolved enantiomers were collected using a Berger MultiGram Prep SFC (Berger Instruments, Inc., Newark, DE) under the following conditions: Chiralpak AD-H SFC column (5 μ m, 250 mm length \times 20 mm i.d., Chiral Technologies, Inc., Exton, PA), 35 °C column

temperature, 10% isopropanol with 0.2% DEA as CO₂ modifier, 50 mL/min flow rate, 100 bar outlet pressure, 220 nm UV detection. The chiral purity of each enantiomer was determined under the same SFC conditions using a Chiralcel OD column (10 μ m, 250 mm length \times 4.6 mm i.d.) at 2.0 mL/min flow rate on a Berger Analytical SFC instrument. The enantiomeric purity of 1-[(1R)-1-(3-chlorophenyl)-2-(dimethylamino)ethyl]cyclohexanol was determined to be >99.9% (with <0.1% of the undesired enantiomer) isolated as peak 2: retention time, 4.69 min; $[\alpha]_D^{25} + 8.8^\circ$ (*c* 10 mg/mL, MeOH). HRMS: calcd for C₁₆H₂₄ClNO + H⁺, 282.161 92; found (ESI, [M + H]⁺), 282.1634.

1-[(1S)-1-(3-Chlorophenyl)-2-(dimethylamino)ethyl]cyclohexanol [(S)-(+)-9**].** The enantiomeric purity was determined to be >99.9% (with <0.1% of the undesired enantiomer) isolated as peak 1: retention time, 3.91 min; $[\alpha]_D^{25} - 10.8^\circ$ (*c* 10 mg/mL, MeOH). HRMS: calcd for C₁₆H₂₄ClNO + H⁺, 282.161 92; found (ESI, [M + H]⁺), 282.1628. Anal. (C₁₆H₂₄ClNO·HCl) C, H, N.

General Procedure for the Synthesis of Aldol Intermediates 14a–j. A solution of diisopropylamine (7.87 mL, 56.2 mmol) in dry tetrahydrofuran (50 mL) under nitrogen was cooled to -78 °C and treated dropwise with a solution of *n*-butyllithium (2.5 M in hexanes, 22 mL, 55 mmol). The resulting solution was warmed to 0 °C and stirred for 15 min. The solution was recooled to -78 °C and treated, via cannula, with a solution of the appropriate phenylacetic acid (23.4 mmol) in tetrahydrofuran (20 mL). The mixture was then allowed to warm to 25 °C where it was stirred for 45 min and was then recooled to -78 °C. A solution of cyclohexanone (3.65 mL, 35.3 mmol) in tetrahydrofuran (10 mL) was then added via cannula, and the resulting mixture was stirred at -78 °C for 1.5 h. The reaction was then quenched by the addition of a saturated aqueous solution of ammonium chloride, and the tetrahydrofuran was removed in vacuo. The resulting residue was dissolved in a 2 N aqueous solution of sodium hydroxide (30 mL) and washed with ethyl acetate (1 \times 30 mL). The aqueous layer was then acidified to pH 1 with the addition of a 2 N aqueous solution of hydrochloric acid. The product was extracted with ethyl acetate (3 \times 30 mL), and the combined organic extracts were dried over magnesium sulfate and concentrated in vacuo to yield product (83–99%) that was used without further purification.

(1-Hydroxycyclohexyl)-4-methoxyphenylacetic Acid 14a. ¹H NMR (DMSO-*d*₆, 400 MHz) δ 1.14–1.15 (m, 2H), 1.34–1.54 (m, 8H), 3.50 (s, 1H), 3.73 (s, 3H), 4.28 (bs, 1H), 6.85 (d, *J* = 8.8 Hz, 2H), 7.32 (d, *J* = 8.8 Hz, 2H), 12.35 (bs, 1H). HRMS: calcd for C₁₅H₂₀O₄ + NH₄⁺, 282.169 98; found (ESI-FT/MS, [M + NH₄]⁺), 282.1706.

(1-Hydroxycyclohexyl)-3-methoxyphenylacetic Acid 14b. ¹H NMR (DMSO-*d*₆, 400 MHz) δ 1.00–1.10 (m, 1H), 1.12–1.21 (m, 1H), 1.31–1.55 (m, 8H), 3.54 (s, 1H), 3.73 (s, 3H), 4.32 (bs, 1H), 6.84 (dd, *J* = 2.1, 8.2 Hz, 1H), 6.96 (d, *J* = 7.8 Hz, 1H), 6.99 (d, *J* = 2.1 Hz, 1H), 7.20 (t, *J* = 7.9 Hz, 1H), 12.32 (bs, 1H). HRMS: calcd for C₁₅H₂₀O₄ + Na⁺, 287.1254; found (ESI-FT/MS, [M + Na]⁺), 287.1256.

4-Fluoro-(1-hydroxycyclohexyl)phenylacetic Acid 14c. ¹H NMR (DMSO-*d*₆, 400 MHz) δ 1.05–1.10 (m, 2H), 1.33–1.57 (m, 8H), 3.59 (s, 1H), 4.31 (bs, 1H), 7.12 (dd, *J* = 2.1, 9.0 Hz, 2H), 7.45 (dd, *J* = 2.2, 8.8 Hz, 2H), 12.43 (bs, 1H). HRMS: calcd for C₁₄H₁₇FO₃ - H⁺, 251.10890; found (ESI, [M - H]⁻), 251.1077.

3-Fluoro-(1-hydroxycyclohexyl)phenylacetic Acid 14d. ¹H NMR (DMSO-*d*₆, 400 MHz) δ 1.06–1.21 (m, 2H), 1.34–1.60 (m, 8H), 3.62 (s, 1H), 4.37 (bs, 1H), 7.09 (dddd, *J* = 0.9, 2.6, 9.0, 9.0 Hz, 1H), 7.22 (d, *J* = 7.8 Hz, 2H), 7.27–7.36 (m, 2H), 12.50 (bs, 1H). HRMS: calcd for C₁₄H₁₇FO₃ - H⁺, 251.10890; found (ESI, [M - H]⁻), 251.1083.

2-Fluoro-(1-hydroxycyclohexyl)phenylacetic Acid 14e. ^1H NMR (CDCl_3 , 400 MHz) δ 1.15–1.28 (m, 2H), 1.35 (d, $J = 13.5$ Hz, 1H), 1.41–1.58 (m, 5H), 7.09 (ddd, $J = 3.6, 10.3, 13.4$ Hz, 1H), 1.86 (dd, $J = 2.6, 14.4$ Hz, 1H), 4.12 (s, 1H), 4.56 (bs, 1H), 7.04–7.13 (m, 2H), 7.25–7.30 (m, 1H), 7.61 (ddd, $J = 1.5, 7.6, 7.6$ Hz, 1H). HRMS: calcd for $\text{C}_{14}\text{H}_{17}\text{FO}_3 - \text{H}^+$, 251.10890; found (ESI, $[\text{M} - \text{H}]^-$), 251.1087. Anal. Calcd for $\text{C}_{14}\text{H}_{17}\text{FO}_3 \cdot 0.5\text{H}_2\text{O}$: C, 64.35; H, 6.94; N, 0.00. Found: C, 64.40; H, 7.04; N, 0.00.

4-Chloro-(1-hydroxycyclohexyl)phenylacetic Acid 14f. ^1H NMR ($\text{DMSO}-d_6$, 400 MHz) δ 1.05–1.21 (m, 2H), 1.33–1.60 (m, 8H), 3.59 (s, 1H), 4.34 (bs, 1H), 7.36 (ddd, $J = 2.6, 2.6, 9.1$ Hz, 2H), 7.45 (ddd, $J = 2.6, 2.6, 9.2$ Hz, 2H), 12.47 (bs, 1H). HRMS: calcd for $\text{C}_{14}\text{H}_{17}\text{ClO}_3 - \text{H}^+$, 267.07935; found (ESI, $[\text{M} - \text{H}]^-$), 267.0792.

3-Chloro-(1-hydroxycyclohexyl)phenylacetic Acid 14g. ^1H NMR ($\text{DMSO}-d_6$, 400 MHz) δ 1.06–1.23 (m, 2H), 1.33–1.56 (m, 8H), 3.61 (s, 1H), 4.37 (bs, 1H), 7.22–7.38 (m, 3H), 7.53 (s, 1H), 12.50 (bs, 1H). HRMS: calcd for $\text{C}_{14}\text{H}_{17}\text{ClO}_3 + \text{Na}^+$, 291.07584; found (ESI-FT, $[\text{M} + \text{Na}]^{1+}$), 291.0748.

(1-Hydroxycyclohexyl)-(4-trifluoromethoxy)phenylacetic Acid 14h. ^1H NMR ($\text{DMSO}-d_6$, 400 MHz) δ 1.06–1.21 (m, 2H), 1.35 (d, $J = 10.4$ Hz, 1H), 1.42–1.58 (m, 7H), 3.64 (s, 1H), 4.37 (bs, 1H), 7.29 (d, $J = 8.5$ Hz, 2H), 7.55 (d, $J = 8.8$ Hz, 2H), 12.51 (bs, 1H). HRMS: calcd for $\text{C}_{15}\text{H}_{17}\text{F}_3\text{O}_4 + \text{H}^+$, 319.11517; found (ESI, $[\text{M} + \text{H}]^+$), 319.1145. Anal. Calcd for $\text{C}_{15}\text{H}_{17}\text{F}_3\text{O}_4 \cdot 0.10\text{H}_2\text{O}$: C, 56.28; H, 5.41; N, 0.00. Found: C, 56.03; H, 4.99; N, 0.00.

(1-Hydroxycyclohexyl)-(3-trifluoromethoxy)phenylacetic Acid 14i. ^1H NMR ($\text{DMSO}-d_6$, 400 MHz) δ 1.10–1.21 (m, 2H), 1.34–1.54 (m, 8H), 3.67 (s, 1H), 4.40 (bs, 1H), 7.27 (d, $J = 3.6$ Hz, 1H), 7.40–7.48 (m, 3H), 12.54 (bs, 1H). HRMS: calcd for $\text{C}_{15}\text{H}_{17}\text{F}_3\text{O}_4 + \text{H}^+$, 319.11517; found (ESI, $[\text{M} + \text{H}]^+$), 319.1158.

(1-Hydroxycyclohexyl)-(3-trifluoromethyl)phenylacetic Acid 14j. ^1H NMR ($\text{DMSO}-d_6$, 400 MHz) δ 1.03–1.23 (m, 2H), 1.30–1.58 (m, 8H), 3.73 (s, 1H), 4.42 (bs, 1H), 7.53 (t, $J = 7.8$ Hz, 1H), 7.62 (dd, $J = 0.7, 7.8$ Hz, 1H), 7.72 (d, $J = 7.7$ Hz, 1H), 12.52 (bs, 1H). HRMS: calcd for $\text{C}_{15}\text{H}_{17}\text{F}_3\text{O}_3 + \text{Na}^+$, 325.10220; found (ESI-FT, $[\text{M} + \text{Na}]^{1+}$), 325.1024.

General Procedure for the Coupling of Aldol Intermediates To Form boc-Protected Amides 15a–j. A solution of aldol intermediate **14a–j** (2.00 mmol), benzotriazol-1-yloxytris(dimethylamino)phosphonium hexafluorophosphate (1.42 g, 3.22 mmol), and *tert*-butyl 1-piperazinecarboxylate (0.60 g, 3.22 mmol) in methylene chloride (20 mL) was treated with triethylamine (0.84 mL, 6.0 mmol). The mixture was stirred at 25 °C for 16 h, after which time the solvent was removed in vacuo and the products (compounds **15a–j**) were purified via Biotage Horizon (FLASH 40 M, silica, gradient from 0% EtOAc/hexane to 30% EtOAc/hexane). This reaction gave a range of yields between 59% and 87%.

***tert*-Butyl 4-[(1-Hydroxycyclohexyl)(4-methoxyphenyl)acetyl]piperazine-1-carboxylate 15a.** ^1H NMR ($\text{DMSO}-d_6$, 400 MHz) δ 0.99–1.19 (m, 3H), 1.31 (s, 9H) 1.31–1.48 (m, 5H), 1.51–1.58 (m, 2H), 2.68–2.76 (m, 1H), 3.04–3.21 (m, 3H), 3.26–3.39 (m, 2H), 3.41–3.48 (m, 1H), 3.52–3.60 (m, 1H), 3.67 (s, 3H), 3.89 (s, 1H), 5.27 (s, 1H), 6.80 (d, $J = 8.8$ Hz, 2H), 7.25 (d, $J = 8.7$ Hz, 2H). HRMS: calcd for $\text{C}_{23}\text{H}_{33}\text{FN}_2\text{O}_4 + \text{CH}_3\text{CO}_2$, 479.2557; found (ESI, $[\text{M} + \text{OAc}]^-$), 479.2548.

***tert*-Butyl 4-[(1-Hydroxycyclohexyl)(3-methoxyphenyl)acetyl]piperazine-1-carboxylate 15b.** ^1H NMR ($\text{DMSO}-d_6$, 400 MHz) δ 1.01–1.20 (m, 3H), 1.37 (s, 9H) 1.37–1.53 (m, 5H), 1.54–1.66 (m, 2H), 2.78–2.85 (m, 1H), 3.11–3.28 (m, 3H), 3.31–3.44 (m, 2H), 3.50–3.57 (m, 1H), 3.61–3.70 (m, 1H), 3.72 (s, 3H), 3.99 (s, 1H), 5.36 (s, 1H), 6.84 (ddd, $J = 1.9, 1.9, 7.6$ Hz, 1H), 6.96–6.98 (m, 2H), 7.21 (t, $J = 7.8$ Hz, 1H). HRMS: calcd for $\text{C}_{23}\text{H}_{33}\text{FN}_2\text{O}_4 + \text{CH}_3\text{CO}_2$, 479.2557; found (ESI, $[\text{M} + \text{OAc}]^-$), 479.2578.

***tert*-Butyl 4-[(4-Fluorophenyl)(1-hydroxycyclohexyl)acetyl]piperazine-1-carboxylate 15c.** ^1H NMR ($\text{DMSO}-d_6$, 400 MHz) δ 0.95–1.02 (m, 1H), 1.05–1.14 (m, 2H), 1.37 (s, 9H) 1.37–1.65 (m, 7H), 2.80–2.88 (m, 1H), 3.16–3.28 (m, 3H), 3.33–3.44 (m, 2H), 3.50–3.58 (m, 1H), 3.61–3.70 (m, 1H), 4.06 (s, 1H), 5.28

(s, 1H), 7.13 (ddd, $J = 2.0, 9.0, 9.0$ Hz, 2H), 7.44 (dd, $J = 5.6, 8.8$ Hz, 2H). HRMS: calcd for $\text{C}_{24}\text{H}_{36}\text{N}_2\text{O}_5 + \text{H}^+$, 433.2697; found (ESI, $[\text{M} + \text{H}]^+$), 433.2703.

***tert*-Butyl 4-[(3-Fluorophenyl)(1-hydroxycyclohexyl)acetyl]piperazine-1-carboxylate 15d.** ^1H NMR ($\text{DMSO}-d_6$, 400 MHz) δ 1.00–1.05 (m, 1H), 1.06–1.19 (m, 2H), 1.37 (s, 9H) 1.37–1.69 (m, 7H), 2.87–2.85 (m, 1H), 3.15–3.24 (m, 3H), 3.31–3.42 (m, 2H), 3.52–3.61 (m, 1H), 3.66–3.74 (m, 1H), 4.10 (s, 1H), 5.27 (s, 1H), 7.09 (dddd, $J = 1.3, 2.6, 9.0, 9.0$ Hz, 1H), 7.25 (dd, $J = 1.3, 9.0$ Hz, 2H), 7.35 (m, 1H). HRMS: calcd for $\text{C}_{23}\text{H}_{33}\text{FN}_2\text{O}_4 + \text{H}^+$, 421.2497; found (ESI, $[\text{M} + \text{H}]^+$), 421.2500.

***tert*-Butyl 4-[(2-Fluorophenyl)(1-hydroxycyclohexyl)acetyl]piperazine-1-carboxylate 15e.** ^1H NMR ($\text{DMSO}-d_6$, 400 MHz) δ 1.11–1.14 (m, 3H), 1.33–1.63 (m, 6H), 1.37 (s, 9H), 1.68–1.74 (m, 1H), 2.73–2.80 (m, 1H), 3.10–3.18 (m, 1H), 3.21–3.30 (m, 2H), 3.41–3.59 (m, 4H), 4.21 (s, 1H), 5.18 (s, 1H), 7.15–7.23 (m, 2H), 7.34 (ddd, $J = 1.0, 7.6, 7.6$ Hz, 1H), 7.54 (ddd, $J = 1.7, 7.8, 7.8$ Hz, 1H). HRMS: calcd for $\text{C}_{23}\text{H}_{33}\text{FN}_2\text{O}_4 + \text{H}^+$, 421.2497; found (ESI, $[\text{M} + \text{H}]^+$), 421.2509. Anal. ($\text{C}_{23}\text{H}_{33}\text{FN}_2\text{O}_4$) C, H, N.

***tert*-Butyl 4-[(4-Chlorophenyl)(1-hydroxycyclohexyl)acetyl]piperazine-1-carboxylate 15f.** ^1H NMR ($\text{DMSO}-d_6$, 400 MHz) δ 0.97–1.03 (m, 1H), 1.05–1.15 (m, 2H), 1.37 (s, 9H) 1.37–1.66 (m, 7H), 2.81–2.90 (m, 1H), 3.12–3.28 (m, 3H), 3.35–3.42 (m, 2H), 3.50–3.58 (m, 1H), 3.61–3.70 (m, 1H), 4.07 (s, 1H), 5.26 (s, 1H), 7.37 (d, $J = 8.6$ Hz, 2H), 7.43 (d, $J = 8.8$ Hz, 2H). HRMS: calcd for $\text{C}_{23}\text{H}_{33}\text{ClN}_2\text{O}_4 + \text{H}^+$, 437.2202; found (ESI, $[\text{M} + \text{H}]^+$), 437.2213.

***tert*-Butyl 4-[(3-Chlorophenyl)(1-hydroxycyclohexyl)acetyl]piperazine-1-carboxylate 15g.** ^1H NMR ($\text{DMSO}-d_6$, 400 MHz) δ 1.03–1.19 (m, 3H), 1.37 (s, 9H) 1.37–1.64 (m, 7H), 2.90–3.00 (m, 1H), 3.21–3.24 (m, 3H), 3.31–3.37 (m, 2H), 3.58–3.62 (m, 1H), 3.69–3.78 (m, 1H), 4.10 (s, 1H), 5.24 (s, 1H), 7.32–7.39 (m, 3H), 7.50 (s, 1H). HRMS: calcd for $\text{C}_{23}\text{H}_{33}\text{ClN}_2\text{O}_4 + \text{H}^+$, 437.2202; found (ESI, $[\text{M} + \text{H}]^+$), 437.2187.

***tert*-Butyl 4-[(1-Hydroxycyclohexyl)[4-(trifluoromethoxy)phenyl]acetyl]piperazine-1-carboxylate 15h.** ^1H NMR ($\text{DMSO}-d_6$, 400 MHz) δ 0.95–1.02 (m, 1H), 1.09–1.18 (m, 2H), 1.37 (s, 9H), 1.37–1.68 (m, 7H), 2.85–2.92 (m, 1H), 3.14–3.24 (m, 3H), 3.30–3.40 (m, 2H), 3.55–3.62 (m, 1H), 3.65–3.72 (m, 1H), 4.13 (s, 1H), 5.25 (s, 1H), 7.31 (d, $J = 8.4$ Hz, 2H), 7.54 (d, $J = 8.7$ Hz, 2H); MS (ESI) m/z 487. Anal. Calcd for $\text{C}_{24}\text{H}_{33}\text{F}_3\text{N}_2\text{O}_5 \cdot 0.40\text{H}_2\text{O}$: C, 58.38; H, 6.90; N, 5.67. Found: C, 57.91; H, 7.02; N, 6.27.

***tert*-Butyl 4-[(1-Hydroxycyclohexyl)[3-(trifluoromethoxy)phenyl]acetyl]piperazine-1-carboxylate 15i.** ^1H NMR ($\text{DMSO}-d_6$, 400 MHz) δ 0.96–1.04 (m, 1H), 1.10–1.19 (m, 2H), 1.37 (s, 9H), 1.38–1.69 (m, 7H), 2.72–2.80 (m, 1H), 3.10–3.30 (m, 3H), 3.39–3.54 (m, 3H), 3.62–3.70 (m, 1H), 4.16 (s, 1H), 5.24 (s, 1H), 7.27 (d, $J = 3.2$ Hz, 1H), 7.41–7.49 (m, 3H). HRMS: calcd for $\text{C}_{24}\text{H}_{33}\text{F}_3\text{N}_2\text{O}_5 + \text{H}^+$, 487.2414; found (ESI, $[\text{M} + \text{H}]^+$), 487.2406.

***tert*-Butyl 4-[(1-Hydroxycyclohexyl)[3-(trifluoromethyl)phenyl]acetyl]piperazine-1-carboxylate 15j.** ^1H NMR ($\text{DMSO}-d_6$, 400 MHz) δ 0.90–0.96 (m, 1H), 1.02–1.12 (m, 2H), 1.31 (s, 9H) 1.32–1.60 (m, 7H), 2.82–2.90 (m, 1H), 3.08–3.18 (m, 3H), 3.28–3.35 (m, 2H), 3.51–3.59 (m, 1H), 3.64–3.71 (m, 1H), 4.18 (s, 1H), 5.17 (s, 1H), 7.49 (t, $J = 7.7$ Hz, 1H), 7.57 (d, $J = 7.7$ Hz, 1H), 7.68 (d, $J = 7.7$ Hz, 1H), 7.75 (s, 1H). HRMS: calcd for $\text{C}_{24}\text{H}_{33}\text{F}_3\text{N}_2\text{O}_4 + \text{H}^+$, 471.2426; found (ESI, $[\text{M} + \text{H}]^+$), 471.2423.

General Procedure for the Separation of Enantiomers To Form Amines (R)-(+)-15g, (S)-(–)-15g, (R)-(+)-15i, (S)-(–)-15i. Racemic boc-protected amides **15g** and **15i** were dissolved in methanol at a concentration of approximately 40 mg/mL, and the resulting solution was injected onto the supercritical fluid chromatography (SFC) instrument with a volume of 1.0 mL per injection. The baseline resolved enantiomers were collected using a Berger MultiGram Prep SFC (Berger Instruments, Inc., Newark, DE) under the following conditions: Chiralpak AD-H SFC column (5 μm , 250 mm length \times 20 mm i.d., Chiral Technologies, Inc., Exton, PA), 35 °C column temperature, 40% methanol as CO_2 modifier for **15g** and 20% methanol as CO_2 modifier for **15i**, 50 mL/min flow rate, 100 bar outlet pressure, 220 nm UV detection. The chiral purity of

each enantiomer was determined under the same SFC conditions using a Chiralpak AD-H column (10 μ m, 250 mm length \times 4.6 mm i.d.) at 2.0 mL/min flow rate on a Berger Analytical SFC instrument.

tert-Butyl 4-[(2R)-2-(3-Chlorophenyl)-2-(1-hydroxycyclohexyl)acetyl]piperazine-1-carboxylate (R)-(+)-15g. The enantiomeric purity of was determined to be 99.5% (with 0.5% of the undesired enantiomer) isolated as peak 1: retention time, 2.82 min; $[\alpha]_D^{25} +14^\circ$ (c 6.2 mg/mL, EtOH). HRMS: calcd for $C_{23}H_{33}ClN_2O_4 + H^+$, 437.2202; found (ESI, $[M + H]^+$), 437.2203.

tert-Butyl 4-[(2S)-2-(3-Chlorophenyl)-2-(1-hydroxycyclohexyl)acetyl]piperazine-1-carboxylate (S)-(-)-15g. The enantiomeric purity of was determined to be 99.6% (with 0.4% of the undesired enantiomer) isolated as peak 2: retention time, 3.84 min; $[\alpha]_D^{25} -24^\circ$ (c 4.6 mg/mL, EtOH). HRMS: calcd for $C_{23}H_{33}ClN_2O_4 + H^+$, 437.2202; found (ESI, $[M + H]^+$), 437.2212.

tert-Butyl 4-[(2R)-2-(1-Hydroxycyclohexyl)-2-[3-(trifluoromethoxy)phenyl]acetyl]piperazine-1-carboxylate (R)-(+)-15i. The enantiomeric purity of was determined to be >99.9% (with <0.1% of the undesired enantiomer) isolated as peak 1: retention time, 3.0 min; $[\alpha]_D^{25} +23^\circ$ (c 11.6 mg/mL, EtOH). HRMS: calcd for $C_{23}H_{33}ClN_2O_4 + CH_3CO_2$, 495.2262; found (ESI, $[M + OAc]^-$), 495.2268.

tert-Butyl 4-[(2S)-2-(1-Hydroxycyclohexyl)-2-[3-(trifluoromethoxy)phenyl]acetyl]piperazine-1-carboxylate (S)-(-)-15i. The enantiomeric purity of was determined to be 99.8% (with 0.2% of the undesired enantiomer) isolated as peak 2: retention time, 3.58 min; $[\alpha]_D^{25} -19^\circ$ (c 11.2 mg/mL, MeOH). HRMS: calcd for $C_{23}H_{33}ClN_2O_4 + CH_3CO_2$, 495.2262; found (ESI, $[M + OAc]^-$), 495.2272.

General Procedure for the Amide Reduction and Deprotection To Form Amines 16a–j. A solution of boc-protected amide (**15a–j**) (0.46 mmol) in dry tetrahydrofuran (3 mL) under nitrogen was treated dropwise with a solution of borane (1.0 M in tetrahydrofuran, 1.60 mL, 1.60 mmol). The resulting solution was heated at 70 $^\circ$ C for 2 h, after which time the mixture was cooled in an ice bath and was treated dropwise with a 2 N aqueous solution of hydrochloric acid (1 mL). The mixture was again heated at 70 $^\circ$ C for 1 h and was then cooled and treated with methanol (1 mL). After the solvent was removed in vacuo, the resulting residue was dissolved in water (5 mL) and was washed with ethyl acetate (1 \times 4 mL). The aqueous layer was basified with the addition of a 2 N aqueous solution of sodium hydroxide until pH 10 was attained. The product was extracted with ethyl acetate (4 \times 5 mL) and the combined organic extracts were dried over magnesium sulfate and concentrated in vacuo to yield the amine as a colorless oil, which was used directly in the next step or converted to the HCl salt for pharmacological testing. The HCl salts were formed by dissolving the product in methanol (0.5 mL) and treating with a saturated methanolic solution of hydrochloric acid (0.5 mL) followed by diethyl ether. After crystallizing in the refrigerator for 16 h, the resulting solid was filtered, washed with diethyl ether, and dried in vacuo to afford the final products (**16a–k**) in a yield range between 51% and 69% as white solids.

1-[1-(4-Methoxyphenyl)-2-piperazin-1-ylethyl]cyclohexanol Dihydrochloride 16a. 1H NMR (D_2O , 400 MHz) δ 0.88–1.00 (m, 1H), 1.09 (d, $J = 12.4$ Hz, 1H), 1.14 (dd, $J = 4.4, 10.9$ Hz, 1H), 1.17–1.40 (m, 6H), 1.56 (d, $J = 12.9$ Hz, 1H), 2.95 (dd, $J = 3.5, 11.3$ Hz, 1H), 3.31–3.50 (m, 8H), 3.60 (dd, $J = 3.5, 13.3$ Hz, 1H), 3.66–3.72 (m, 1H), 3.68 (s, 3H), 6.88 (d, $J = 9.0$ Hz, 2H), 7.20 (d, $J = 8.3$ Hz, 2H). HRMS: calcd for $C_{19}H_{30}N_2O_2 + H^+$, 319.2380; found (ESI, $[M + H]^+$), 319.2376. Anal. Calcd for $C_{19}H_{30}N_2O_2 \cdot 2HCl \cdot 1.2H_2O$: C, 55.26; H, 8.40; N, 6.78. Found: C, 55.48; H, 8.8; N, 6.67.

1-[1-(3-Methoxyphenyl)-2-piperazin-1-ylethyl]cyclohexanol Dihydrochloride 16b. 1H NMR (D_2O , 400 MHz) δ 0.90–0.99 (m, 1H), 1.10–1.12 (m, 1H), 1.17–1.37 (m, 7H), 1.59 (d, $J = 12.2$ Hz, 1H), 2.99 (d, $J = 10.5$ Hz, 1H), 3.18 (s, 1H), 3.32–3.42 (m, 7H), 3.64 (d, $J = 13.3$ Hz, 1H), 3.69 (s, 3H), 3.77 (t, $J = 12.2$ Hz, 1H), 6.84–6.90 (m, 3H), 7.24 (t, $J = 7.8$ Hz, 1H). Anal. Calcd for

$C_{19}H_{30}N_2O_2 \cdot 2HCl \cdot 0.5H_2O$: C, 57.00; H, 8.31; N, 7.00. Found: C, 57.31; H, 8.64; N, 6.89.

1-[1-(4-Fluorophenyl)-2-piperazin-1-ylethyl]cyclohexanol Dihydrochloride 16c. 1H NMR ($DMSO-d_6$, 400 MHz) δ 1.02–1.16 (m, 2H), 1.20–1.24 (m, 2H), 1.32–1.35 (m, 1H), 1.44–1.64 (m, 5H), 3.29–3.80 (m, 11H), 4.62 (s, 1H) 7.18 (d, $J = 7.3$ Hz, 2H), 7.39 (bs, 2H), 9.46 (bs, 2H), 10.60 (bs, 1H). HRMS: calcd for $C_{18}H_{27}FN_2O + H^+$, 307.2180; found (ESI, $[M + H]^+$), 307.2166. Anal. Calcd for $C_{18}H_{27}FN_2O \cdot 2HCl \cdot 1.0H_2O$: C, 54.41; H, 7.86; N, 7.05. Found: C, 54.51; H, 7.88; N, 7.06.

1-[1-(3-Fluorophenyl)-2-piperazin-1-ylethyl]cyclohexanol Dihydrochloride 16d. 1H NMR (D_2O , 400 MHz) δ 0.89–1.00 (m, 1H), 1.08 (d, $J = 12.2$ Hz, 1H), 1.16 (dd, $J = 4.5, 10.9$ Hz, 1H), 1.20–1.37 (m, 6H), 1.60 (d, $J = 13.2$ Hz, 1H), 3.04 (dd, $J = 3.1, 11.1$ Hz, 1H), 3.21–3.55 (m, 8H), 3.65 (dd, $J = 3.2, 13.5$ Hz, 1H), 3.75 (t, $J = 11.1$ Hz, 1H), 7.98 (dd, $J = 2.1, 8.3$ Hz, 1H), 7.02 (t, $J = 7.3$ Hz, 1H), 7.07 (d, $J = 7.7$ Hz, 1H), 7.98 (ddd, $J = 6.3, 8.1, 8.1$ Hz, 1H). HRMS: calcd for $C_{18}H_{27}FN_2O + H^+$, 307.2180; found (ESI, $[M + H]^+$), 307.2179. Anal. Calcd for $C_{18}H_{27}FN_2O \cdot 2HCl \cdot 1.3H_2O$: C, 53.68; H, 7.91; N, 6.96. Found: C, 53.97; H, 8.2; N, 7.02.

1-[1-(2-Fluorophenyl)-2-piperazin-1-ylethyl]cyclohexanol Dihydrochloride 16e. 1H NMR (D_2O , 400 MHz) δ 0.88–0.98 (m, 1H), 1.16–1.47 (m, 8H), 1.64 (d, $J = 12.9$ Hz, 1H), 3.28–3.50 (m, 9H), 3.67 (dd, $J = 3.2, 13.3$ Hz, 1H), 3.70–3.80 (m, 1H), 7.05 (ddd, $J = 1.2, 8.3, 8.3$ Hz, 1H), 7.13 (t, $J = 7.5$ Hz, 1H), 7.13 (dddd, $J = 1.7, 5.4, 7.3, 7.3$ Hz, 1H), 7.30–7.36 (m, 1H). HRMS: calcd for $C_{18}H_{27}FN_2O + H^+$, 307.2180; found (ESI, $[M + H]^+$), 307.2166. Anal. Calcd for $C_{18}H_{27}FN_2O \cdot 2.00HCl \cdot 1.0H_2O$: C, 54.41; H, 7.86; N, 7.04. Found: C, 54.52; H, 8.05; N, 6.80.

1-[1-(4-Chlorophenyl)-2-piperazin-1-ylethyl]cyclohexanol Dihydrochloride 16f. 1H NMR (D_2O , 400 MHz) δ 1.09–1.12 (m, 1H), 1.24 (d, $J = 12.9$ Hz, 1H), 1.30 (dd, $J = 4.8, 10.9$ Hz, 1H), 1.29–1.60 (m, 6H), 1.74 (d, $J = 12.9$ Hz, 1H), 3.14 (dd, $J = 3.5, 10.9$ Hz, 1H), 3.41–3.49 (m, 8H), 3.71 (dd, $J = 3.5, 13.4$ Hz, 1H), 3.77 (t, $J = 13.4$ Hz, 1H), 7.38 (d, $J = 8.5$ Hz, 2H), 7.45 (d, $J = 8.7$ Hz, 2H). HRMS: calcd for $C_{18}H_{27}ClN_2O + H^+$, 323.1885; found (ESI, $[M + H]^+$), 323.1868. Anal. Calcd for $C_{18}H_{27}ClN_2O \cdot 2.00HCl \cdot 1.0H_2O$: C, 52.24; H, 7.56; N, 6.77. Found: C, 52.27; H, 8.0; N, 6.72.

1-[1-(3-Chlorophenyl)-2-piperazin-1-ylethyl]cyclohexanol Dihydrochloride 16g. 1H NMR for free base ($DMSO-d_6$, 400 MHz) δ 0.94–1.14 (m, 3H), 1.37–1.56 (m, 7H), 2.28 (bs, 2H), 2.33 (bs, 2H), 2.43 (dd, $J = 6.2, 12.4$ Hz, 1H), 2.59 (t, $J = 4.7$ Hz, 4 H), 2.93 (t, $J = 6.4, 1$ H), 3.01 (dd, $J = 8.1, 12.4$ Hz, 1H), 5.31 (s, 1H), 7.18 (d, $J = 7.3$ Hz, 1H), 7.22–7.29 (m, 3H); 1H NMR for dihydrochloride salt (D_2O , 400 MHz) δ 0.89–1.00 (m, 1H), 1.07 (d, $J = 12.8$ Hz, 1H), 1.15 (dd, $J = 4.6, 11.0$ Hz, 1H), 1.20–1.41 (m, 6H), 1.60 (d, $J = 12.7$ Hz, 1H), 3.00 (dd, $J = 3.2, 11.1$ Hz, 1H), 3.18–3.51 (m, 8H), 3.62 (dd, $J = 3.2, 13.5$ Hz, 1H), 3.71 (t, $J = 11.1$ Hz, 1H), 7.18 (d, $J = 6.8$ Hz, 1H), 7.23–7.32 (m, 3H). HRMS: calcd for $C_{18}H_{27}ClN_2O + H^+$, 323.1885; found (ESI, $[M + H]^+$), 323.18831. Anal. Calcd for $C_{18}H_{27}ClN_2O \cdot 2.00HCl \cdot 1H_2O$: C, 52.24; H, 7.56; N, 6.77. Found: C, 52.00; H, 7.36; N, 6.78.

1-[(1R)-1-(3-Chlorophenyl)-2-piperazin-1-ylethyl]cyclohexanol Dihydrochloride (R)-(-)-16g. $[\alpha]_D^{25} -7^\circ$ (c 5.1 mg/mL, MeOH). HRMS: calcd for $C_{18}H_{27}ClN_2O + H^+$, 323.1885; found (ESI, $[M + H]^+$), 323.1873.

1-[(1S)-1-(3-Chlorophenyl)-2-piperazin-1-ylethyl]cyclohexanol Dihydrochloride (S)-(+)-16g. $[\alpha]_D^{25} +12.5^\circ$ (c 4.5 mg/mL, MeOH). HRMS: calcd for $C_{18}H_{27}ClN_2O + H^+$, 323.1885; found (ESI, $[M + H]^+$), 323.1867. Anal. Calcd for $C_{18}H_{27}ClN_2O \cdot 2.00HCl \cdot 1.0H_2O$: C, 52.24; H, 7.56; N, 6.77. Found: C, 52.23; H, 7.37; N, 6.65.

1-[2-Piperazin-1-yl-1-[4-(trifluoromethoxy)phenyl]ethyl]cyclohexanol Dihydrochloride 16h. 1H NMR ($DMSO-d_6$, 400 MHz) δ 1.02 (t, $J = 11.6$ Hz, 2H), 1.15 (d, $J = 13.6$ Hz, 1H), 1.22 (t, $J = 11.1$ Hz, 1H), 1.31–1.36 (m, 1H), 1.45 (dd, $J = 2.3, 12.2$ Hz, 3H), 1.55 (t, $J = 12.2$ Hz, 1H), 1.67 (d, $J = 13.0$ Hz, 1H), 3.10–3.81 (m, 11H), 4.53 (bs, 1H), 7.33 (d, $J = 8.1$ Hz, 2H), 7.49 (d, $J = 8.5$ Hz, 2H), 9.70 (bs, 2H), 11.01 (bs, 1H). HRMS: calcd

for $C_{19}H_{27}F_3N_2O_2 + H^+$, 373.2097; found (ESI, $[M + H]^+$), 373.2086. Anal. Calcd for $C_{19}H_{27}F_3N_2O_2 \cdot 2.00HCl \cdot 2.10 H_2O$: C, 47.23; H, 6.93; N, 5.80. Found: C, 46.93; H, 6.80; N, 5.41.

1-[2-Piperazin-1-yl-1-[3-(trifluoromethoxy)phenyl]ethyl]cyclohexanol Dihydrochloride 16i. 1H NMR (D_2O , 400 MHz) δ 0.86–1.00 (m, 1H), 1.08 (d, $J = 13.1$ Hz, 1H), 1.14 (dd, $J = 4.9$, 10.9 Hz, 1H), 1.19–1.37 (m, 6H), 1.60 (d, $J = 13.1$ Hz, 1H), 3.06 (dd, $J = 3.2$, 11.0 Hz, 1H), 3.31–3.49 (m, 8H), 3.66 (dd, $J = 3.0$, 13.5 Hz, 1H), 3.75 (t, $J = 13.3$ Hz, 1H), 7.19–7.21 (m, 2H), 7.25 (d, $J = 7.7$ Hz, 1H), 7.36 (t, $J = 7.9$ Hz, 1H). HRMS: calcd for $C_{19}H_{27}F_3N_2O_2 + H^+$, 373.2097; found (ESI, $[M + H]^+$), 373.2095. Anal. Calcd for $C_{19}H_{27}F_3N_2O_2 \cdot 2.00HCl \cdot 1.5H_2O$: C, 48.31; H, 6.83; N, 5.93. Found: C, 48.45; H, 6.79; N, 5.76.

1-[(1R)-2-Piperazin-1-yl-1-[3-(trifluoromethoxy)phenyl]ethyl]cyclohexanol Dihydrochloride (R)-(-)-16i. $[\alpha]_D^{25} -4.5^\circ$ (c 10.2 mg/mL, MeOH). HRMS: calcd for $C_{19}H_{27}F_3N_2O_2 + H^+$, 373.2097; found (ESI, $[M + H]^+$), 373.2102.

1-[(1S)-2-Piperazin-1-yl-1-[3-(trifluoromethoxy)phenyl]ethyl]cyclohexanol Dihydrochloride (S)-(+)-16i. $[\alpha]_D^{25} +2.2^\circ$ (c 9.9 mg/mL, MeOH). HRMS: calcd for $C_{19}H_{27}F_3N_2O_2 + H^+$, 373.2097; found (ESI, $[M + H]^+$), 373.2094.

1-[2-Piperazin-1-yl-1-[3-(trifluoromethyl)phenyl]ethyl]cyclohexanol Dihydrochloride 16j. 1H NMR (D_2O , 400 MHz) δ 0.89–1.00 (m, 1H), 1.05 (d, $J = 11.5$ Hz, 1H), 1.12–1.37 (m, 7H), 1.62 (d, $J = 13.1$ Hz, 1H), 3.10 (d, $J = 10.6$ Hz, 1H), 3.30–3.39 (m, 8H), 3.61–3.68 (m, 1H), 3.64 (dd, $J = 3.0$, 13.5 Hz, 1H), 3.77 (dd, $J = 11.4$, 13.2 Hz, 1H), 7.43–7.49 (m, 2H), 7.57–7.59 (m, 2H). HRMS: calcd for $C_{19}H_{27}F_3N_2O + H^+$, 357.2148; found (ESI, $[M + H]^+$), 357.2155.

General Procedure for N-Methylation To Form N-Methylpiperazines 17a–j. A solution of the appropriate amine (**16a–j**) (0.17 mmol) in formic acid (0.33 mL) at 50 °C was treated with an aqueous solution of formaldehyde (37% in water, 0.14 mL, 0.21 mmol). The mixture was heated at 70 °C for 1.5 h, after which time the mixture was poured into water (5 mL) and basified to pH 10 with the addition of a 2 N aqueous solution of sodium hydroxide. The product was then extracted with ethyl acetate (3 \times 4 mL), and the combined organic extracts were dried over magnesium sulfate and concentrated to yield the methylamine as a colorless oil. The product was dissolved in methanol (0.5 mL), and the resulting solution was treated with a saturated methanolic solution of hydrochloric acid (0.5 mL) followed by diethyl ether (2 mL). The solution was stored in the refrigerator for 16 h. The resulting precipitate was filtered and washed with diethyl ether to afford the dihydrochloride salt (compounds **17a–j**) in a yield range of 58–79% as a white solid.

1-[1-(4-Methoxyphenyl)-2-(4-methyl-1-piperazinyl)ethyl]cyclohexanol Dihydrochloride 17a. 1H NMR (D_2O , 400 MHz) δ 0.99–1.08 (m, 1H), 1.19 (d, $J = 12.9$ Hz, 1H), 1.20–1.50 (m, 7H), 1.65 (d, $J = 13.1$ Hz, 1H), 2.88 (s, 3H), 3.04 (dd, $J = 3.3$, 11.0 Hz, 1H), 3.47 (bs, 8H), 3.70 (dd, $J = 3.4$, 12.9 Hz, 1H), 3.75–3.81 (m, 1H), 3.78 (s, 3H), 6.97 (d, $J = 8.7$ Hz, 2H), 7.29 (d, $J = 8.3$ Hz, 2H). Anal. ($C_{20}H_{32}N_2O_2 \cdot 2.00HCl$) C, H, N.

1-[1-(3-Methoxyphenyl)-2-(4-methyl-1-piperazinyl)ethyl]cyclohexanol Dihydrochloride 17b. 1H NMR (D_2O , 400 MHz) δ 1.01–1.10 (m, 1H), 1.20–1.22 (m, 1H), 1.25–1.53 (m, 7H), 1.69 (d, $J = 12.5$ Hz, 1H), 2.90 (s, 3H), 3.08 (dd, $J = 2.8$, 11.5 Hz, 1H), 3.30–3.52 (m, 8H), 3.74 (dd, $J = 2.9$, 12.1 Hz, 1H), 3.77–3.83 (m, 1H), 3.79 (s, 3H), 6.95–7.01 (m, 3H), 7.36 (t, $J = 8.1$ Hz, 1H). Anal. ($C_{20}H_{32}N_2O_2 \cdot 2.00HCl$) C, H, N.

1-[1-(4-Fluorophenyl)-2-(4-methylpiperazin-1-yl)ethyl]cyclohexanol Dihydrochloride 17c. 1H NMR (D_2O , 400 MHz) δ 1.09–1.19 (m, 1H), 1.24 (d, $J = 13.2$ Hz, 1H), 1.28–1.56 (m, 7H), 1.73 (d, $J = 12.5$ Hz, 1H), 2.87 (s, 3H), 3.10 (dd, $J = 3.6$, 10.9 Hz, 1H), 3.22–3.50 (m, 8H), 3.58 (dd, $J = 3.5$, 13.3 Hz, 1H), 3.65 (t, $J = 13.2$ Hz, 1H), 7.16 (t, $J = 8.9$ Hz, 2H), 7.39 (dd, $J = 5.6$, 8.5 Hz, 2H). HRMS: calcd for $C_{19}H_{29}FN_2O + H^+$, 321.2337; found (ESI, $[M + H]^+$), 321.2332. Anal. ($C_{19}H_{29}FN_2O \cdot 2.00HCl$) C, H, N.

1-[1-(3-Fluorophenyl)-2-(4-methylpiperazin-1-yl)ethyl]cyclohexanol Dihydrochloride 17d. 1H NMR (D_2O , 400 MHz) δ 1.10–1.13 (m, 1H), 1.25 (d, $J = 12.0$ Hz, 1H), 1.30–1.56 (m, 7H), 1.74 (d, $J = 12.5$ Hz, 1H), 2.88 (s, 3H), 3.12 (dd, $J = 3.4$, 10.9 Hz, 1H), 3.22–3.50 (m, 8H), 3.57 (dd, $J = 3.2$, 13.2 Hz, 1H), 3.65 (t, $J = 13.2$ Hz, 1H), 7.10–7.16 (m, 1H), 7.20 (d, $J = 7.6$ Hz, 2H), 7.42 (q, $J = 8.1$ Hz, 1H). HRMS: calcd for $C_{19}H_{29}FN_2O + H^+$, 321.2337; found (ESI, $[M + H]^+$), 321.2328. Anal. ($C_{19}H_{29}FN_2O \cdot 2.00HCl$) C, H, N.

1-[1-(2-Fluorophenyl)-2-(4-methylpiperazin-1-yl)ethyl]cyclohexanol Dihydrochloride 17e. 1H NMR (D_2O , 400 MHz) δ 1.03 (bs, 1H), 1.28–1.52 (m, 8H), 1.74 (d, $J = 12.6$ Hz, 1H), 2.89 (s, 3H), 3.47 (bs, 9H), 3.70–3.88 (m, 2H), 7.16 (t, $J = 8.4$ Hz, 1H), 7.23 (t, $J = 7.5$ Hz, 1H), 7.37 (q, $J = 5.8$ Hz, 1H), 7.46 (bs, 1H). HRMS: calcd for $C_{19}H_{29}FN_2O + H^+$, 321.2337; found (ESI, $[M + H]^+$), 321.2326. Anal. Calcd for $C_{19}H_{29}FN_2O \cdot 2.00HCl \cdot 0.1H_2O$: C, 57.74; H, 7.95; N, 7.09. Found: C, 57.61; H, 7.43; N, 6.78.

1-[1-(4-Chlorophenyl)-2-(4-methylpiperazin-1-yl)ethyl]cyclohexanol Dihydrochloride 17f. 1H NMR (D_2O , 400 MHz) δ 1.09–1.12 (m, 1H), 1.24 (d, $J = 13.3$ Hz, 1H), 1.28–1.56 (m, 7H), 1.73 (d, $J = 12.5$ Hz, 1H), 2.89 (s, 3H), 3.10 (dd, $J = 3.5$, 10.7 Hz, 1H), 3.22–3.55 (m, 8H), 3.60 (dd, $J = 3.5$, 13.4 Hz, 1H), 3.65 (t, $J = 13.4$ Hz, 1H), 7.37 (d, $J = 8.4$ Hz, 2H), 7.44 (d, $J = 8.7$ Hz, 1H). HRMS: calcd for $C_{19}H_{29}ClN_2O + H^+$, 337.2041; found (ESI, $[M + H]^+$), 337.2060. Anal. Calcd for $C_{19}H_{29}ClN_2O \cdot 2.00HCl \cdot 0.3H_2O$: C, 54.96; H, 7.67; N, 6.75. Found: C, 55.26; H, 7.37; N, 6.68.

1-[1-(3-Chlorophenyl)-2-(4-methylpiperazin-1-yl)ethyl]cyclohexanol Dihydrochloride 17g. 1H NMR for free base (DMSO- d_6 , 400 MHz) δ 0.96–1.07 (m, 1H), 1.08–1.14 (m, 2H), 1.31–1.59 (m, 7H), 2.10 (s, 3H), 2.22 (bs, 4H), 2.38 (bs, 4H), 2.47 (dd, $J = 6.8$, 12.5 Hz, 1H), 2.90 (t, $J = 7.0$ Hz, 1H), 3.04 (ddd, $J = 7.5$, 9.5, 12.6 Hz, 1H), 5.12 (s, 1H), 7.18 (dd, $J = 1.5$, 7.2 Hz, 1H), 7.21–7.28 (m, 3H). HRMS: calcd for $C_{19}H_{29}ClN_2O + H^+$, 337.2041; found (ESI, $[M + H]^+$), 337.2036. Anal. ($C_{19}H_{29}ClN_2O \cdot 2.00HCl$) C, H, N.

1-[(1R)-1-(3-Chlorophenyl)-2-(4-methylpiperazin-1-yl)ethyl]cyclohexanol Dihydrochloride (R)-(+)-17g. The enantiomeric purity was determined to be >99.9% (with <0.1% of the undesired enantiomer): retention time, 2.49 min; $[\alpha]_D^{25} +29^\circ$ (c 9.9 mg/mL, MeOH). HRMS: calcd for $C_{19}H_{29}ClN_2O + H^+$, 337.2041; found (ESI, $[M + H]^+$), 337.2032. Anal. ($C_{19}H_{29}ClN_2O \cdot 2.00HCl$) C, H, N.

1-[(1S)-1-(3-Chlorophenyl)-2-(4-methylpiperazin-1-yl)ethyl]cyclohexanol Dihydrochloride (S)-(-)-17g. The enantiomeric purity was determined to be >99.9% (with <0.1% of the undesired enantiomer): retention time, 3.58 min; $[\alpha]_D^{25} -21.4^\circ$ (c 10 mg/mL, MeOH). HRMS: calcd for $C_{19}H_{29}ClN_2O + H^+$, 337.2041; found (ESI, $[M + H]^+$), 337.2032. Anal. Calcd for $C_{19}H_{29}ClN_2O \cdot 2.00HCl \cdot 0.2H_2O$: C, 55.20; H, 7.66; N, 6.78. Found: C, 55.24; H, 7.85; N, 6.67.

1-[2-(4-Methylpiperazin-1-yl)-1-[4-(trifluoromethoxy)phenyl]ethyl]cyclohexanol Dihydrochloride 17h. 1H NMR (D_2O , 400 MHz) δ 1.00–1.09 (m, 1H), 1.20–1.50 (m, 7H), 1.68 (d, $J = 12.9$ Hz, 1H), 2.89 (s, 3H), 3.12 (dd, $J = 2.8$, 10.9 Hz, 1H), 3.47 (bs, 8H), 3.72 (d, $J = 13.2$ Hz, 1H), 3.80 (t, $J = 11.1$ Hz, 1H), 7.30 (d, $J = 8.1$ Hz, 2H), 7.42 (d, $J = 8.3$ Hz, 2H). HRMS: calcd for $C_{20}H_{29}F_3N_2O_2 + H^+$, 387.2254; found (ESI, $[M + H]^+$), 387.2245.

1-[2-(3-Methylpiperazin-1-yl)-1-[3-(trifluoromethoxy)phenyl]ethyl]cyclohexanol Dihydrochloride 17i. 1H NMR (D_2O , 400 MHz) δ 0.96–0.98 (m, 1H), 1.09–1.43 (m, 8H), 1.62 (d, $J = 12.6$ Hz, 1H), 2.81 (s, 3H), 3.06 (dd, $J = 3.2$, 10.9 Hz, 1H), 3.38 (bs, 8H), 3.64 (dd, $J = 3.2$, 13.5 Hz, 1H), 3.74 (dd, $J = 11.0$, 13.4 Hz, 2H), 7.21–7.28 (m, 3H), 7.38 (t, $J = 8.5$ Hz, 1H). HRMS: calcd for $C_{20}H_{29}F_3N_2O_2 + H^+$, 387.2254; found (ESI, $[M + H]^+$), 387.2263.

1-[(1R)-2-(4-Methylpiperazin-1-yl)-1-[3-(trifluoromethoxy)phenyl]ethyl]cyclohexanol Dihydrochloride (R)-(+)-17i. The enantiomeric purity was determined to be >99.8% (with 0.2% of the undesired enantiomer): retention time, 9.52 min; $[\alpha]_D^{25} +20.6^\circ$ (c 10.8 mg/mL, MeOH). HRMS: calcd for $C_{20}H_{29}F_3N_2O_2 + H^+$,

387.2254; found (ESI, $[M + H]^+$), 387.2269. Anal. ($C_{20}H_{29}F_3N_2O_2 \cdot 2.00HCl$) C, H, N.

1-[(1S)-2-(4-Methylpiperazin-1-yl)-1-[3-(trifluoromethoxy)phenyl]ethyl]cyclohexanol Dihydrochloride (S)-(-)-17i. The enantiomeric purity was determined to be >99.9% (with <0.1% of the undesired enantiomer): retention time, 7.85 min; $[\alpha]_D^{25} -25.1^\circ$ (*c* 10 mg/mL, MeOH). HRMS: calcd for $C_{20}H_{29}F_3N_2O_2 + H^+$, 387.2254; found (ESI, $[M + H]^+$), 387.2249. Anal. ($C_{20}H_{29}F_3N_2O_2 \cdot 2.00HCl$) C, H, N.

1-{2-(3-Methylpiperazin-1-yl)-1-[3-(trifluoromethyl)phenyl]ethyl}cyclohexanol Dihydrochloride 17j. 1H NMR (D_2O , 400 MHz) δ 0.93–0.99 (m, 1H), 1.05 (d, *J* = 12.6 Hz, 1H), 1.13 (dd, *J* = 4.6, 11.1 Hz, 1H), 1.17–1.37 (m, 6H), 1.62 (d, *J* = 12.9 Hz, 1H), 2.79 (s, 3H), 3.09 (dd, *J* = 3.1, 10.9 Hz, 1H), 3.38 (bs, 8H), 3.66 (d, *J* = 13.5 Hz, 1H), 3.78 (t, *J* = 13.3 Hz, 1H), 7.45 (t, *J* = 7.7 Hz, 1H), 7.50 (d, *J* = 7.6 Hz, 2H), 7.57–7.59 (m, 2H). HRMS: calcd for $C_{20}H_{29}F_3N_2O + H^+$, 371.2305; found (ESI, $[M + H]^+$), 371.2290. Anal. Calcd for $C_{20}H_{29}F_3N_2O \cdot 2.00HCl \cdot 0.3H_2O$: C, 53.53; H, 7.10; N, 6.24. Found: C, 53.60; H, 7.22; N, 6.21.

General Procedure for Whole Cell Radioligand Binding Assay in Cells Expressing Human Norepinephrine Transporter (hNET). Twenty-four hours prior to assay, MDCK-Net6 cells stably transfected with human NET²¹ were plated in 96-well plates at 3000–5000 cells/well in growth medium and maintained in a cell incubator (37 °C, 5% CO₂). On day 2, growth medium was replaced with 80 μ L of assay buffer (25 mM HEPES, 120 mM NaCl, 5 mM KCl, 2.5 mM CaCl₂, 1.2 mM MgSO₄, 2 mg/mL glucose (pH 7.4, 37 °C)) containing 0.2 mg/mL ascorbic acid and 1 μ M pargyline. Ten microliter aliquots of test compound in assay buffer were added directly to triplicate wells to yield final test concentrations of 10–10000 nM. Data from wells containing desipramine (1 μ M) were used to define nonspecific hNET binding (minimum hNET binding in the presence of an NRI). Total radioligand bound was defined by addition of 5 μ L of binding buffer alone in the presence of [³H]nisoxetine. The radioligand binding reaction was initiated by addition of [³H]nisoxetine in 25 μ L of assay buffer to each well for a final concentration of 3 nM. The total and nonspecific cpm values obtained for this assay were 2849 \pm 69 and 188 \pm 3.5, respectively. The *K*_D value estimated for [³H]nisoxetine was 10 nM using intact whole cells. Test compounds and cells were preincubated at 37 °C for 15 min prior to initiating the binding reaction by addition of radioligand. The cells in the assay buffer with test compound and radioligand were incubated for 2 h at 37 °C. The cells were washed twice with 200 μ L of assay buffer at room temperature to remove unbound radioligand. After binding, cells were incubated for 1 h in Microscint20 scintillation fluid (PerkinElmer Life and Analytical Sciences, Boston, MA) and radiolabeled ligand binding quantified using a TopCount plate scintillation counter (PerkinElmer). Each compound was tested in two separate experiments at a minimum and up to four times in some cases.

General Procedure for Norepinephrine (NE) Uptake Assay in Cells Expressing Human Norepinephrine Transporter (hNET). On day 1, MDCK-Net6 cells, stably transfected with human NET,²² were plated at 3000 cells/well in a 96-well plate in growth medium and maintained in a cell incubator (37 °C, 5% CO₂). On day 2, growth medium was replaced with 80 μ L of assay buffer (25 mM HEPES, 120 mM NaCl, 5 mM KCl, 2.5 mM CaCl₂, 1.2 mM MgSO₄, 2 mg/mL glucose [pH 7.4, 37 °C]) containing 0.2 mg/mL ascorbic acid and 10 μ M pargyline. Cells were equilibrated in 90 μ L of assay buffer for 10 min at 37 °C prior to addition of compounds. A stock solution of desipramine was prepared in DMSO (10 mM) and delivered to triplicate wells containing cells for a final test concentration of 200 nM. Data from these wells were used to define nonspecific NE uptake (minimum NE uptake). Test compound stock solutions were prepared in DMSO/water (1:1) (10 mM) and diluted in assay buffer according to test range (1–10000 nM). A 10 μ L aliquot of vehicle or various concentrations of antagonist was added directly to triplicate wells containing cells in 80 μ L of assay buffer. The cells were preincubated with test compound for 15 min at 37 °C. To initiate uptake, [³H]NE (1-

[7,8-³H]norepinephrine, ~30 Ci/mmol from Amersham Biosciences) was diluted in assay buffer (50 nM final assay concentration) and delivered in 10 μ L aliquots to each well and the plates were incubated for 10 min at 37 °C. Medium was then removed from wells, and cells were washed twice with 200 μ L assay buffer to remove unincorporated [³H]NE label. The wells containing cells were then incubated for 1 h in 80 μ L of Microscint20 scintillation fluid (PerkinElmer Life and Analytical Sciences, Boston, MA), and the [³H]NE accumulation was quantified using a Topcount scintillation counter (PerkinElmer). By use of the above detailed assay conditions, the typical *K*_m value for [³H]NE was 534 \pm 92 nM and the *V*_{max} value was 5.5 \pm 0.9 pmol/well. The total and nonspecific cpm values obtained for these assays are 9415 \pm 191 and 213 \pm 7.1, respectively. Each compound was tested in two separate experiments at a minimum and up to four times in some cases.

General Procedure for Serotonin (hSERT) Uptake Assay in Cells Expressing Human Serotonin Transporter. On day 1, JAR cells (human placental choriocarcinoma), purchased from ATCC (catalog no. HTB-144), were plated at 15 000 cells/well in 96-well plates containing growth medium (RPMI 1640 with 10% FBS) and maintained in a cell incubator (37 °C, 5% CO₂). On day 2, cells were stimulated with staurosporine (40 nM) to increase the expression of the 5-HT transporter.²³ On day 3, cells were removed from the cell incubator 2 h prior to assay and maintained at room temperature to equilibrate the growth medium to ambient oxygen concentration. Subsequently, the growth medium was replaced with 200 μ L of assay buffer (25 mM HEPES, 120 mM NaCl, 5 mM KCl, 2.5 mM CaCl₂, 1.2 mM MgSO₄, 2 mg/mL glucose (pH 7.4, 37 °C)) containing 0.2 mg/mL ascorbic acid and 1 μ M pargyline, and the cells were incubated for 5 min at 37 °C. A stock solution of paroxetine (AHR-4389-1) was prepared in DMSO (10 mM) and delivered to triplicate wells containing cells for a final test concentration of 1 μ M. Data from these wells were used to define nonspecific 5-HT uptake (minimum 5-HT uptake in the presence of a SRI). Test compounds were prepared in DMSO/water (1:1) (10 mM) and diluted in assay buffer according to test range (1–1000 nM). An amount of 25 μ L of assay buffer (maximum 5-HT uptake) or test compound was added directly to triplicate wells containing cells in 200 μ L of assay buffer. The cells were incubated with the compound for 10 min (37 °C). To initiate the reaction, [³H]hydroxytryptamine creatinine sulfate diluted in assay buffer was delivered in 25 μ L aliquots to each well for a final test concentration of 15 nM. The cells were incubated with the reaction mixture for 9 min at 37 °C. Decanting the supernatant from the plates terminated the reaction. The cells were washed twice with 200 μ L of assay buffer (37 °C) to remove free radioligand. The plates were inverted and left to dry for 2 min, then reinverted and air-dried for an additional 10 min. Subsequently, the cells were lysed in 25 μ L of 0.25 N NaOH (4 °C) and then placed on a shaker table and shaken vigorously for 5 min. After cell lysis, 75 μ L of scintillation cocktail was added to the wells and the plates were sealed with film tape and replaced on the shake table for a minimum of 10 min. The plates were counted in a Wallac Microbeta counter (PerkinElmer) to collect the raw cpm data. By use of the above detailed assay conditions, the typical *K*_m value for [³H]hydroxytryptamine creatinine sulfate was 431 \pm 86.2 nM and the *V*_{max} value was 11.5 \pm 1.2 pmol/well. The total and nonspecific cpm values obtained for this assay are 4282 \pm 206 and 79 \pm 5.5, respectively. Each compound was tested in two separate experiments at a minimum and up to four times in some cases.

General Procedure for the Dopamine Transporter (hDAT) Membrane Binding Assay. Frozen membrane samples from CHO cells expressing recombinant hDAT, purchased from Perkin-Elmer, Boston, MA (catalog no. RBHDATM, lot no. 2227), were diluted to 7.5 mL in binding buffer (50 mM Tris-HCl, pH 7.4, 100 mM NaCl), homogenized with a tissue-tearer (Polytron PT 1200C, Kinematica AG), and delivered at a volume of 75 μ L to each well of a polypropylene 96-well plate. The binding reaction was carried out in polypropylene 96-well plates (Costar General Assay Plate, catalog no. 3359; Lid, catalog no. 3930). Homogenized membrane preparation was delivered at a volume of 75 μ L to each well of a

reaction plate. A stock solution of mazindol was prepared in DMSO (10 mM) and delivered to triplicate wells containing membranes for a final test concentration of 10 μ M. Mazindol has been reported to be a dopamine transporter inhibitor (DRI)²⁴ with an IC₅₀ value of 20.5 nM in our assays. Data from wells containing mazindol (10 μ M) were used to define nonspecific (NSB) hDAT binding (minimum hDAT binding in the presence of a DRI). Total radioligand bound was defined by addition of 5 μ L of binding buffer alone in the presence of radioligand **18**. Stock solutions of test compounds were prepared in DMSO/water (1:1) at a concentration of 10 mM. On day of assay, the test compound stock solution was diluted in assay buffer according to test range (3000–100000 nM) ensuring a maximal DMSO concentration of less than 0.5% in the assay reaction wells. Homogenized membranes were preincubated with test compound for 20 min at 4 °C before the initiation of the binding reaction. The binding reaction was initiated by addition of 25 μ L of radioligand **18** diluted in binding buffer. The final concentration of radioligand **18** delivered was 32 nM. The K_D value estimated for radioligand **18** (lot no. 2227) in hDAT membranes was 29.7 nM. The plates containing the radioligand binding reactions were incubated for 2 h at 4 °C on a shaking table (Bellco, Vineland, NJ) at 3 rpm. The MultiScreen-FB opaque 96-well filtration plates containing Millipore glass fiber filters (Millipore glass fiber B, catalog no. MAFBN0B) were used to terminate the binding reactions and to separate bound from free radioligand. The plates were presoaked with 0.5% polyethylenimine (PEI, Sigma catalog no. P-3143) in water for a minimum of 2 h at room temperature to reduce nonspecific binding of radioligand **18** during the harvest procedure. Prior to harvesting of the reaction plates, the PEI solution was aspirated from the filter plates using a vacuum manifold. Aliquots of each mixture (90 μ L of each 100 μ L reaction well) were transferred from the reaction plates to the filter plates using a Zymark Rapid Plate-96 automated pipet station. The binding reaction was terminated by vacuum filtration through the glass fiber filters. The filter plates were aspirated at 5–10 in. Hg, and the wells are washed 9 times with 200 μ L of wash buffer (50 mM Tris-HCl, 0.9% NaCl, pH 7.4, 4 °C) using a 12-channel aspiration/wash system. Plastic bottom supports were removed from the filter plates, and the plates were placed in plastic liners. A 100 μ L aliquot of scintillation fluid was added to each well, and the top of each plate was sealed with adhesive film. The plates were vigorously shaken on an orbital shake table (Bellco) at 5 rpm for 10–15 min to ensure adequate equilibration of aqueous to solvent partitioning. The collection of raw cpm data was done using a Wallac Microbeta counter (Perkin-Elmer). The total and nonspecific cpm values obtained for this assay were 1976.3 \pm 52.8 and 95.7 \pm 3.2, respectively.

Procedure for the Tail Suspension Test in Mice. Male Swiss Webster mice (Charles River Laboratories, MA) weighing 20–35 g (2–3 months of age) were used for the study. Experimental groups consisted of 10 mice, randomly assigned to drug or vehicle (2% Tween-80/0.5% methylcellulose) treatment. The procedure followed in this study was a variant to the original report by Steru et al.^{13a} Thirty minutes following administration of (*S*)-(-)-**17i** (10, 17, and 30 mg/kg, ip) the mice were suspended upside down by the tail using adhesive laboratory tape (VWR International, PA) to a flat metal bar connected to a strain gauge within a tail suspension chamber (Med Associates, VT). The time spent immobile during a 6 min test session was automatically recorded. Eight mice were simultaneously tested in separate chambers. Data collected were expressed as a mean of immobility time, and statistical analysis was performed using a one-way ANOVA with least significant difference (LSD) post hoc test. Data represent group mean values \pm SEM for each dose (*N* = 10 per group).

Procedure for the *p*-Phenylquinone (PPQ) Model of Acute Visceral Pain. Male CD-1 mice (Charles River; Kingston/Ston-eridge, NY) weighing 20–25 g were maintained on a 12 h light/dark cycle (lights on at 0630) in groups of five on corn cob bedding, and food and water were available ad libitum. Experimental groups consisted of eight mice randomly assigned to drug or vehicle (saline) treatment. The ability of compounds to attenuate acute visceral

(abdominal) pain was assessed following an ip injection of 2 mg/kg PPQ (dissolved in 4–6% ethanol/distilled water). Following PPQ injection, mice were individually placed in a Plexiglas cage and the number of stretching movements was recorded during two 1 min periods, 5 and 10 min after injection. Compound (*S*)-(-)-**17i** (3, 10, and 30 mg/kg, sc) and desipramine (3, 10 and 30 mg/kg, sc) were administered 60 min prior to PPQ injection. Statistical analysis was done using a one-way ANOVA on raw data (total number of stretches). Significant main effects were analyzed further by subsequent least significant difference analysis. The criterion for significant differences was *p* < 0.05. Data are presented as percent blockade compared to vehicle (% blockade = [(mean vehicle) – (drug)]/(mean vehicle) \times 100).

Procedure for the OVX-Induced Thermoregulatory Dysfunction Telemetry Rat Model. Tail-skin temperature (TST) was measured by a temperature and physical activity transmitter (PhysioTel TA10TA-F40, Data Sciences International) that was implanted subcutaneously in the dorsal scapular region of ovariectomized female SD rats. The tip of the temperature probe was tunneled subcutaneously 2.5 cm beyond the base of the tail. After a 7-day recovery period, rats were administered vehicle (2% Tween-80/0.5% methylcellulose), and TST was monitored continuously for 12 h (during the dark cycle). Twenty-four hours later rats were administered either vehicle or test compound and TST was monitored continuously for 12 h (during the dark cycle). All vehicle and test compounds were administered 1 h prior to the onset of the dark cycle. Test compound alterations in TST were analyzed using a 2 day paradigm. For both the vehicle (baseline) and compound testing, TST was recorded at 5 min intervals and an average TST was calculated for every 30 min time point. On day 1, an overall average baseline TST was established for each individual animal by taking the mean over the 12 h observation period. On day 2, test compound was administered and TST readings were reported as an average over every 30 min as described above. All data were analyzed as Δ TST (TST for each time point on day 2 minus average baseline TST for day 1). A one-way ANOVA was performed to obtain the average within-group standard deviation. For each 30 min interval, a *t* test was performed and evaluated to determine if the average Δ TST was statistically different (*p* \geq 0.05) from baseline.

Acknowledgment. The authors thank members of the Discovery Analytical Chemistry group in Chemical Technologies at Wyeth, particularly Scott Brecker, Christopher Petucci, Rebecca Dooley, Diane Andraka, and Oliver McConnell for compound analysis. Their efforts and dedication are greatly appreciated. We also thank our management, Drs. M. Abou-Gharbia, R. Magolda, L. Freedman, and M. Pangalos for their support of this work.

Supporting Information Available: Crystallographic information in cif format, elemental analysis and purity results for all compounds tested in biological assays, raw data from rat telemetry studies, and data and procedures for pharmacokinetic studies. This material is available free of charge via the Internet at <http://pubs.acs.org>.

References

- (1) (a) Devilbiss, D. M.; Page, M. E.; Waterhouse, B. D. Locus coeruleus regulates sensory encoding by neurons and networks in waking animals. *J. Neurosci.* **2006**, *26*, 9860–9872. (b) Aston-Jones, G.; Cohen, J. D. Adaptive gain and the role of the locus coeruleus-norepinephrine system in optimal performance. *J. Comp. Neurol.* **2005**, *493*, 99–110. (c) Valentino, R. J.; Van Bockstaele, E. J. Functional interactions between stress neuromediators and the locus coeruleus-norepinephrine system. *Tech. Behav. Neurosci.* **2005**, *15*, 465–486. (d) Cirelli, C.; Tononi, G. Locus coeruleus control of state-dependent gene expression. *J. Neurosci.* **2004**, *24*, 5410–5419. (e) Miyawaki, T.; Kawamura, H.; Komatsu, K.; Yasugi, T. Chemical stimulation of the locus coeruleus: inhibitory effects on hemodynamics and renal sympathetic nerve activity. *Brain Res.* **1991**, *568*, 101–108.

- (2) Sarvey, J. Protein synthesis in long-term potentiation and norepinephrine-induced long-lasting potentiation in hippocampus. *Neurol. Neurobiol.* **1998**, *35*, 329–353 and references therein.
- (3) (a) Fricchione, G.; Stefano, G. B. Placebo neural systems: nitric oxide, morphine and the dopamine brain reward and motivation circuitries. *Med. Sci. Monit.* **2005**, *11*, MS54–MS65. (b) Kalivas, P. W.; Volkow, N.; Seamans, J. Unmanageable motivation in addiction: a pathology in prefrontal-accumbens glutamate transmission. *Neuron* **2005**, *45*, 647–650. (c) Pochon, J. B.; Levy, R.; Fossati, P.; Lehericy, S.; Poline, J. B.; Pillon, B.; Le Bihan, D.; Dubois, B. The neural system that bridges reward and cognition in humans: an fMRI study. *Proc. Natl. Acad. Sci. U.S.A.* **2002**, *99*, 5669–5674.
- (4) (a) Kumar, V. N. Interrelation between thermoregulation and sleep regulation. *Proc. Natl. Acad. Sci., India, Sect. B* **2003**, *69*, 507–524. (b) Riedel, W.; Dorward, P. K.; Korner, P. I. Central adrenoceptors modify hypothalamic thermoregulatory patterns of autonomic activity in conscious rabbits. *Auton. Neurosci.* **1981**, *3*, 525–533. (c) Lahti, H.; Pyornila, A.; Hissa, R. The influence of 6-OHDA on hypothermia produced by intrahypothalamically-injected carbachol in the pigeon. *Experientia* **1980**, *36*, 1188.
- (5) (a) Michel, M. C.; Ruhe, H. G.; de Groot, A. A.; Castro, R.; Oelke, M. Tolerability of amine uptake inhibitors in urologic diseases. *Curr. Drug Safety* **2006**, *1*, 73–85. (b) Michel, M. C.; Oelke, M. Duloxetine in the treatment of stress urinary incontinence. *Women's Health* **2005**, *1*, 345–348. (c) Osborne, K. L.; Davis, S. M. Duloxetine in the treatment of stress urinary incontinence. *J. Pharm. Technol.* **2005**, *21*, 337–340. (d) McCormack, P. L.; Keating, G. M. Duloxetine: in stress urinary incontinence. *Drugs* **2004**, *64*, 2567–2573.
- (6) (a) Preskorn, S. H.; Ross, R. Other Antidepressants. *Handb. Exp. Pharmacol.* **2004**, *157*, 263–324. (b) Carminati, G. G.; Deriaz, N.; Bertschy, G. Low dose venlafaxine in three adolescents and young adults with autistic disorder improves self-injurious behavior and attention deficit/hyperactivity disorders (ADHD)-like symptoms. *Prog. Neuropsychopharmacol. Biol. Psychiatry* **2006**, *30*, 312–315.
- (7) (a) Arnold, L. M.; Lu, Y.; Crofford, L. J.; Wohleisch, M.; Detke, M. J.; Iyengar, S.; Goldstein, D. J. A double-blind, multicenter trial comparing duloxetine with placebo in the treatment of fibromyalgia patients with or without major depressive disorder. *Arthritis Rheum.* **2004**, *50*, 2974–2984. (b) Arnold, L. M.; Rosen, A.; Pritchett, Y. L.; D'Souza, D. N.; Goldstein, D. J.; Iyengar, S.; Wernicke, J. F. A randomized, double-blind, placebo-controlled trial of duloxetine in the treatment of women with fibromyalgia with or without major depressive disorder. *Pain* **2005**, *119*, 5–15. (c) Sayar, K.; Aksu, G.; Ak, I.; Tosun, M. Venlafaxine treatment of fibromyalgia. *Ann. Pharmacother.* **2003**, *37*, 1561–1565.
- (8) Bymaster, F. P.; Katner, J. S.; Nelson, D. J.; Hemrick-Luecke, S. K.; Threlkeld, P. J.; Heiligenstein, J. H.; Morin, S. M.; Gehlert, D. R.; Perry, K. W. Atomoxetine increases extracellular levels of norepinephrine and dopamine in the prefrontal cortex of rat: a potential mechanism for efficacy in attention hyperactivity disorder. *Neuropsychopharmacology* **2002**, *27*, 699–711.
- (9) (a) Krell, H. V.; Leuchter, A. F.; Cook, I. A.; Abrams, M. Evaluation of reboxetine, a noradrenergic antidepressant, for the treatment of fibromyalgia and chronic low back pain. *Psychosomatics* **2005**, *46*, 379–384. (b) Berigan, T. Use of atomoxetine adjunctively in fibromyalgia syndrome. *Can. J. Psychiatry* **2004**, *49*, 499–500.
- (10) Yardley, J. P.; Husbands, G. E. M.; Stack, Gary, Butch, J.; Bicksler, J.; Moyer, J. A.; Muth, E. A.; Andree, T.; Fletcher, H.; James, M. N. G.; Sielecki, A. R. 2-Phenyl-2-(1-hydroxycycloalkyl)ethylamine derivatives: synthesis and antidepressant activity. *J. Med. Chem.* **1990**, *33*, 2899–2905.
- (11) Mason, J. N.; Deecher, D. C.; Richmond, R. L.; Stack, G.; Mahaney, P. E.; Trybulski, E. J.; Winneker, R. C.; Blakely, R. D. Desvenlafaxine succinate identifies novel antagonist binding determinants in the human norepinephrine transporter. *J. Pharmacol. Exp. Ther.* **2007**, *323*, 720–729.
- (12) (a) Reith, M. E. A.; Meisler, B. E.; Sershen, H.; Lajtha, A. Structural requirements for cocaine congeners to interact with dopamine and serotonin uptake sites in mouse brain and to induce stereotyped behavior. *Biochem. Pharmacol.* **1986**, *35*, 1123–1129. (b) Madras, B. K.; Fahey, M. A.; Borgman, J.; Canfield, D. R.; Spealman, R. D. Effects of cocaine and related drugs in nonhuman primates. I. [³H]Cocaine binding sites in caudate-putamen. *J. Pharmacol. Exp. Ther.* **1989**, *251*, 131–141.
- (13) (a) Steru, L.; Chermat, R.; Thierry, B.; Simon, P. The tail suspension test: a new method for screening antidepressants in mice. *Psychopharmacology* **1985**, *85*, 367–370. (b) Porsolt, R. D.; Chermat, R.; Lenegre, A.; Avril, I.; Janvier, S.; Steru, L. Use of the automated tail suspension test for the primary screening of psychotropic agents. *Arch. Int. Pharmacodyn. Ther.* **1987**, *288*, 11–30. (c) Teste, J. F.; Martin, I.; Rinjard, P. Electrotherapy in mice: dopaminergic and noradrenergic effects in the tail suspension test. *Fundam. Clin. Pharmacol.* **1990**, *4*, 39–47. (d) Cryan, J. F.; Mombereau, C.; Vassout, A. The tail suspension test as a model for assessing antidepressant activity: review of pharmacological and genetic studies in mice. *Neurosci. Biobehav. Rev.* **2005**, *29*, 571–625.
- (14) Ripoll, N.; David, J. P.; Dailly, E.; Hascoet, M.; Bourin, M. Antidepressant-like effects in various mice strains in the tail suspension test. *Behav. Brain Res.* **2003**, *143*, 193–200.
- (15) Siegmund, E.; Cadmus, R.; Lu, G. A method for evaluating both non-narcotic and narcotic analgesics. *Proc. Soc. Exp. Biol. Med.* **1957**, *95*, 279–731.
- (16) (a) Zhou, M.; Gebhart, G. F. Spinal serotonin receptors mediate descending facilitation of a nociceptive reflex from the nuclei reticularis gigantocellularis and gigantocellularis pars alpha in the rat. *Brain Res.* **1991**, *550*, 35–48. (b) Holden, J. E.; Schwartz, E. J.; Proudfit, H. K. Microinjection of morphine in the A7 catecholamine cell group produces opposing effects on nociception that are mediated by alpha-1 and alpha-2-adrenoceptors. *Neuroscience* **1999**, *91*, 979–990.
- (17) (a) Gebhart, G. Modulatory Effects of Descending Systems on Spinal Dorsal Horn Neurons. In *Spinal Afferent Processing*; Yaksh, T. L., Ed.; Plenum: New York, 1986; pp 391–416. (b) Fields, H. L.; Heinricher, M. M.; Mason, P. Neurotransmitters in nociceptive modulatory circuits. *Annu. Rev. Neurosci.* **1991**, *14*, 219–245. (c) Fields, H. L.; Basbaum, A. Central Nervous System Mechanisms of Pain Modulation. In *Textbook of Pain*; Wall, P. D., Melzack, R., Eds.; Churchill Livingstone: London, 1999; pp 309–329. (d) Millan, M. J. Descending control of pain. *Prog. Neurobiol.* **2002**, *66*, 355–474.
- (18) Leventhal, L.; Smith, V.; Hornby, G.; Andree, T. H.; Brandt, M. R.; Rogers, K. E. Differential and synergistic effects of selective norepinephrine and serotonin reuptake inhibitors in rodent models of pain. *J. Pharmacol. Exp. Ther.* **2007**, *320*, 1178–1186.
- (19) (a) Berendsen, H. H.; Weekers, A. H.; Kloosterboer, H. J. Effect of tibolone and raloxifene on the tail temperature of oestrogen-deficient rats. *Eur. J. Pharmacol.* **2001**, *419*, 47–54. (b) Sipe, K.; Leventhal, L.; Burroughs, K.; Cosmi, S.; Johnston, G. H.; Deecher, D. C. Serotonin 2A receptors modulate tail-skin temperature in two rodent models of estrogen deficiency-related thermoregulatory dysfunction. *Brain Res.* **2004**, *1028*, 191–202.
- (20) (a) Deecher, D. C.; Alfinito, P.; Leventhal, L.; Johnston, G. H.; Cosmi, S.; Merchenthaler, I.; Winneker, R. Alleviation of thermoregulatory dysfunction with the new serotonin and norepinephrine reuptake inhibitor desvenlafaxine succinate in ovariectomized rodent models. *Endocrinology* **2007**, *148*, 1376–1383. (b) Maswood, N.; Alfinito, P. D.; Cosmi, S.; Leventhal, L.; Johnston, G. H.; Deecher, D. C. Evaluation of the selective serotonin reuptake inhibitor, fluoxetine, in ovariectomized (OVX) rat models of temperature regulation. *Neuroendocrinology* **2006**, *85*, 330–338.
- (21) Pawlyk, A. C.; Cosmi, S.; Alfinito, P. D.; Maswood, N.; Deecher, D. C. Effects of the 5-HT_{2A} antagonist mirtazapine in rat models of thermoregulation. *Brain Res.* **2006**, *1123*, 135–144.
- (22) Pacholczyk, T.; Blakely, R. D.; Amara, S. G. Expression cloning of a cocaine- and antidepressant-sensitive human noradrenergic transporter. *Nature* **1991**, *350*, 350–354.
- (23) Ramamoorthy, J. D.; Ramamoorthy, S.; Papapetropoulos, A.; Catravas, J. D.; Leibach, F. H.; Ganapathy, V. Cyclic AMP-independent up-regulation of the human serotonin transporter by staurosporine in choriocarcinoma cells. *J. Biol. Chem.* **1995**, *270*, 17189–17195.
- (24) Pristupa, Z. B.; Wilson, J. M.; Hoffman, B. J.; Kish, S. J.; Niznik, H. B. Pharmacological heterogeneity of the cloned and native human dopamine transporter: disassociation of [³H]WIN 35,428 and [³H]GBR 12,935 binding. *Mol. Pharmacol.* **1994**, *45*, 125–35.